Applied Thermal Engineering 174 (2020) 115259

Contents lists available at ScienceDirect

Applied Thermal Engineering

journal homepage: www.elsevier.com/locate/apthermeng

Stability of nanofluid: A review

Samarshi Chakraborty, Pradipta Kumar Panigrahi*

Department of Mechanical Engineering, Indian Institute of Technology Kanpur, India

HIGHLIGHTS

- Stability of nanofluid is a critical factor which influences its applicability.
- Significant research gap exists in implementation of different stabilization techniques.
- Wall effect on stability should be considered in microfluidics and porous media application.
- Salinity effect must be considered for EOR application of nanofluid.
- More studies on hybrid nanofluid stability and quantum dots are warranted.

ARTICLE INFO

Keywords:
Nanofluid
Stability mechanism
Stabilization techniques
Stability evaluation
Quantum dot
Temperature/Salinity/Shearing effect

ABSTRACT

Nanofluid is a suspension of nanoparticles (at least one dimension less than 100 nm) in a basefluid having superior thermal, rheological and wettability properties, which improves the performance of several applications i.e. heat transfer, lubrication, drug delivery and enhanced oil recovery etc. However, the critical bottleneck for widespread use of nanofluid is its stability. The instability of nanofluid leads to reduction in system performance with passage of time. Addressing the long term stability of nanofluid and its reusability are essential requirements for successful industrial use. This article focuses on different aspects of nanofluid stability starting from the preparation stage till implementation in practical applications. Specific attention has been given on nanofluid stability as a function of operating conditions i.e. high temperature, pressure, confinement, composition, salinity, external magnetic field and shear rate etc. in several applications i.e. heat transfer, microfluidics, lubrication, enhanced oil recovery and drag reduction etc. It is expected that the present review will provide guidance and contribute towards wider adoption of nanofluid in practical applications. Future research on stability issues related to techno-economic performance, hybrid nanofluid, quantum dot, hybrid stabilization technique, wall effect in microfluidics and porous media will further enhance the usability of nanofluid in widespread practical systems.

1. Introduction

Nanofluid is a suspension of nanoparticles (at least one dimension below 100 nm) in a base-fluid i.e. water, alcohol, oil and refrigerant etc. In the past three decades, nanofluid has garnered immense attention in the domain of nanotechnology, thermal engineering and several other applications. Quantitative evidence of thermal conductivity enhancement and improved heat transfer performance of different nanofluids has been reported by several researchers [1–5]. Xuan and Li [6] and Yu et al. [4] reported 78% and 34% increase in thermal conductivity using Cu-water and Fe_3O_4–kerosene nanofluid respectively. Similarly, the drag reduction or lubrication aspects of nanofluid have been reported in literature [7,8]. Nakhchi et al. [7] observed friction factor reduction by 23.6% using Cu-water nanofluid in a circular pipe. Implementation of nanofluid has also resulted in enhanced oil recovery (EOR) under saline environment. Suleimanov et al. [9] reported 12–17% enhancement in oil recovery using Sodium Dodecyl Benzene Sulphonate (SDBS) stabilized nonferrous metal nanofluid and Zhang et al. [10] reported 33% increase in EOR using silica nanofluid.

Liquids with suspended particles are prone to destabilization and form sediments as it is subjected to various forces such as Van der Waal attractive force, gravitational force, buoyancy force and electrostatic repulsive force. The Van der Waal attractive force and gravitational force work against the stability of any colloidal suspension. The functionality and performance of nanofluids (suspension of nanoparticle in base fluid) for various applications are highly dependent on its stability. Nanoparticles present in the suspension collide with each other and induce agglomeration of the suspended particles leading to large cluster

* Corresponding author.
E-mail addresses: samarshi.chem@gmail.com (S. Chakraborty), panig@iitk.ac.in (P.K. Panigrahi).

https://doi.org/10.1016/j.applthermaleng.2020.115259
Received 11 December 2019; Received in revised form 10 March 2020; Accepted 26 March 2020
Available online 04 April 2020
1359-4311/

Nomenclature

Symbols

A	Hamekar constant (J)
A_{plate}	Area of interacting plate (m^2)
a	Characteristic radius (nm)
a_s	Radius of sphere (nm)
a_c	Radius of cylinder (nm)
A_λ	Spectral absorbance
c	Concentration of particle (mole/litre)
D	Translational diffusion coefficient
D_p	Diameter of particle (nm)
e	Single electron charge (C)
G_A	Gibbs free energy of attraction (J)
G_{ST}	Gibbs free energy of steric repulsion (J)
G_{OS}	Gibbs free energy of osmotic repulsion (J)
G_{VR}	Gibbs free energy of volume restraint interaction (J)
I	Intensity of laser light beam (cd)
k_B	Boltzman constant (J/K)
L	Length of cylinder (nm)
l	Length of light path (cm)
n	Number density of ionic species in the solution
R_H	Hydrodynamic Radius (nm)
S	Particle separation distance (nm)
T	Absolute temperature (K)
T_λ	Spectral transmittance (%)
V_A	Attractive Interaction Potential (J)
V_R	Repulsive Interaction Potential (J)
V_T	Total Interaction Potential (J)
V_t	Terminal settling velocity (m/s)
X	Distance between axis of rotation and specific location of the tube inside centrifuge (cm)
Z_i	Ions valency

Greek Letters

α	Absorptivity (mol/cm)
ε	Dielectric constant of basefluid
ε_O	Permittivity of vacuum (F/m)
κ	Debye length (nm)
φ	Surface potential (mV)
μ	Viscosity of basefluid (Pa·s)
ρ_p	Density of nanoparticle (kg/m^3)
ρ_o	Density of base fluid (kg/m^3)
ω	Angular velocity of centrifuge (s^{-1})
ζ	Zeta potential (mV)

Abbreviations

AA	Acrylic Acid
AFM	Atomic Force Microscopy
AMPS	2-Acrylamido-2-Methyl-1-Propanesulfonic Acid
CTAB	Cetyl trimethyl ammonium bromide
CTAC	Cetrimonium Chloride
DLS	Dynamic Light Scattering
DLVO	Derjaguin Landau Vewey and Overbeek
DR	Drag Reduction
EDL	Electrical Double Layer
EOR	Enhanced Oil Recovery
FTIR	Fourier-Transform Infrared Spectroscopy
GA	Gum Arabic
HPMC	Hydroxypropylmethylcellulose
IEP	Isoelectric Point
LDH	Layered Double Hydroxide
MFS	Melamine Formaldehyde Sulfonate
MWCNT	Multiwall Carbon Nanotube
PVP	Polyvinylpyrrolidone
PPF	Price Performance Factor
SANSS	Submerged Arc Nanoparticle Synthesis System
SDS	Sodium Dodecyl Sulphate
SDBS	Sodium Dodecyl Benzene Sulphonate
TCR	Thermal Conductivity Ratio
TEM	Transmittance Electron Microscope
VEROS	Vacuum Evaporation on Running Oil Substrate

formation. The tendency of nanoparticles to form cluster in the suspended state leads to destabilization of nanofluid. The nanoparticle suspension shows agglomeration tendency due to its high surface activity. Such agglomeration tendency has to be eliminated for a nanofluid to be considered stable. For stability of nanofluid, the nanoparticles suspended in the basefluid (water, oil, alcohol etc.), should not form large aggregates leading to sedimentation of nanoparticle from the basefluid. According to DLVO theory, when Van der Waal attractive potential dominates over electrostatic repulsive potential, particles tend to agglomerate and eventually lead to sedimentation [11]. The sedimentation of nanoparticles can lead to clogging of microchannel, which limits the successful operation of the microfluidic device and negate the beneficial attributes of nanofluid. The thermo-physical properties (thermal conductivity, viscosity etc.) of nanofluid are dependent on its stability. Poor stability of nanofluid can hinder its performance in several applications such as heat exchanger (increase dirt factor), biomedical application, enhanced oil recovery etc. Particle aggregation and sedimentation may also lead to increase in viscosity, pumping cost and poor thermal properties, which are detrimental for its applicability. In addition, the operational conditions in practical applications i.e. temperature, concentration, salinity, shearing and magnetic field can also adversely influence the stability of nanofluid. Therefore, there is a need to understand the stability aspect of nanofluid starting from preparation, evaluation, stabilization methods and operational aspects.

Comprehensive review of the nanofluid stability has been carried out and reported in the following sequence; (a) classification of nanofluid, (b) nanofluid preparation method, (c) stability evaluation techniques, (d) stability mechanism, (e) factors responsible for nanofluid stability, (f) stabilization methods, and (g) operational conditions effect on stability. There is specific focus on the stability aspect of nanofluid under different operating conditions i.e. temperature, flow condition, porosity, salinity, external magnetic field, wall effect, and shearing etc. The present study emphasizes on identification and explanation of different factors, which can adversely affect the nanofluid stability i.e. dielectric constant of basefluid, zeta potential, pH value, size, shape, and concentration of particle. Instead of overemphasizing on the thermo-physical aspects of nanofluid, the current review concentrates on nanofluid stability. Consideration on stability aspects of nanofluid is expected to improve the wide spread usability of nanofluid.

2. Classification of nanofluid

Based on the types of nanoparticle used for nanofluid synthesis, nanofluid can be classified into four distinctive categories: (a) metal based, (b) metal oxide based, (c) carbon based and, (d) hybrid/mixed metal based. These nanoparticles are suspended in basefluid i.e. water, methanol, ethylene glycol, kerosene, transformer oil, etc. for the formation of nanofluid. Selection of nanofluid for any application should consider not only the improvement in its physical properties but also its stability. A brief summary of each type of nanofluids from stability

Table 1
Summary of different types of nanofluid along with their preparation method and stability indicators (duration and zeta potential).

Nanofluid	Primary Particle Size (nm)	Dispersant	Preparation Method	Stability Duration (h); Zeta Potential (mV)	Reference
Metal based nanofluid					
Ag-Oil	5	Oleic Acid, N-Oleylamine (Steric)	Two-step	720 h	Li et al. [5]
Cu-Water	25	SDBS (Electrostatic)	Two-Step	−43.8 mV	Wang et al. [22]
Au-Water	7.1–12.1	None	Two-step	720 h 32–38.5 mV	Kim et al. [23]
Metal-oxide based nanofluid					
ZnO-EG	10–20	None	Two-Step	6 h	Yu et al. [24]
Fe_3O_4-Kerosene	15	Oleic Acid (Steric)	Two-StepPhase transfer Technique	6 h	Yu et al. [4]
Fe_3O_4-Water	20	Nonylphenol Ethoxylate (Steric)	Two-step	504 h −32 mV	Salari et al. [25]
Al_2O_3-Methanol	40–50	None	Two-Step	60 mV	Pang et al. [26]
Al_2O_3-Water	25	SDBS (Electrostatic)	Two-step	−40.1 mV	Wang et al. [22]
CuO-DI Water	50	HCl + NaOH: pH adjustment & SDS (Electrostatic)	Two-step	1080 h & −11.94 mV	Nikkhah et al. [27]
CuO-Ethylene Glycol (EG)	50	HCl + NaOH: pH adjustment & SDS (Electrostatic)	Two-step	1080 h	Sarafraz et al. [28]
CuO-EG	40–50	SDS (Electrostatic) pH 10.2	Two-step	1800 h	Kamalgharibi et al. [29]
CuO-Water	40–50	pH control method pH 10.2	Two-step	1080 h	Kamalgharibi et al. [29]
TiO_2-Water	40–50	HCl + NaOH: pH adjustment & Triton X-100 (Steric)	Two-step	600 h	Sarafraz et al. [30]
TiO_2-DI Water	40–50	SDS (Electrostatic)	Two-step	264 h	Salari et al. [31]
TiO_2-Water	95 95	None PVP (Steric)	Two-Step Two-step	2 h 8 h	Chakraborty et al. [32]
Carbon based nanofluid					
Functionalized Graphene Oxide-Water	–	$K_2S_2O_8$, KOH, (Electrostatic)	Two-Step' alkaline method	168 h	Ghozatloo et al. [33]
Graphene-water-ethylene glycol WEG = 60:40	Length = 3 μm Thickness = 123–424 nm	HCl + NaOH: pH control & NPE 400 (Electrostatic)	Two-step	504 h	Sarafraz et al. [34]
CNT-Water	Length = 5 μm Diameter = 5–20 nm	SDBS (Electrostatic)	Two-Step	720 h	Wusiman et al. [2]
CNT-Decane	Length = 30 μm Diameter = 15 nm	Oleylamine (Steric)	Two-Step	1440 h	Xie et al. [16]
COOH-CNT-Water	Length = 1.5–2 μm Diameter = 10–20 nm	Nonylphenol ethoxylate (Steric)	Two-step	504 h	Sarafraz et al. [35]
MWCNT-Water	Length = 5–15 μm Diameter = 10 nm	GA (Steric)	Two-Step	720 h −29.1 mV	Indhuja et al. [3]
Hybrid nanofluid					
Al_2O_3-MWCNT-Water	Al_2O_3 Diameter = 30–50 nm MWCNT Length = 5 μm, Diameter = 20 nm	None	Two-Step	120 h	Nine et al. [17]
Nanodiamond-Fe_3O_4-Water	21.2	None	Two-Step	72 h −34.6 mV	Syam Sundar et al. [20]
Ag-MWCNT-Water	Ag Diameter = 80–90 nm MWCNT Length = 5 μm, Diameter = 20 nm	None	One-Step	40 h	Munkhbayar et al. [18]
Cu-Al LDH-Water	Length = 46–68 nm Thickness = 10 nm	None	One-Step	52 mV	Chakraborty et al. [21]
Cu-Zn-Al LDH-Water	Length = 49 nm Thickness = 9 nm	None	One-Step	38.6 mV	Chakraborty et al. [36]
Cu-Zn-Al LDH-Water	Length = 49 nm Thickness = 9 nm	SDS (Electrostatic)	One-Step	−52.7 mV	Chakraborty et al. [37]

perspective are discussed in the following sections.

2.1. Metal based nanofluid

Metallic nanoparticles (Cu, Ag, Au etc.) are suspended in basefluid to prepare metal based nanofluid. Khoshvaght-Aliabadi et al. [12] investigated Cu-nanoparticles suspended in water for heat transfer applications. Li et al. [5] studied the stability and thermal conductivity of oleic acid coated Ag nanoparticles in oil medium and reported 720 h of stability duration. Several other researchers have also studied the stability aspects of metal based nanofluid. Summary on the stability, particle size and synthesis method of different metal based nanofluids are reported in Table 1. It is observed that stable metal based nanofluid can be prepared using two-step method and appropriate stabilizers.

2.2. Metal oxide based nanofluid

The cost of a metallic nanoparticle is the main deterrent behind its widespread industrial applicability. Metal oxide nanoparticles (TiO_2, Fe_3O_4, ZnO, Al_2O_3 etc.) provide an economical alternative. Therefore, most used type of nanofluid is the metal oxide based nanofluid. Table 1 reports the summary of various studies on the stability of metal oxide based nanofluids, which demonstrates different range of stability depending on the type of nanofluid and preparation method.

2.3. Carbon based nanofluid

The carbon based nanofluids display significant enhancement in thermal properties compared to base fluid. However, its high cost limits widespread commercial use. Bulk of articles on carbon based nanofluid (Graphene, GO, CNT etc.) have generally discussed about its thermal conductivity [13], electrical conductivity [14], and applications [15]. Only few selected articles have discussed about its stability aspects in different basefluids (water, ethylene glycol, propyl glycol, liquid paraffin, oil etc.). Xie et al. [16] reported 1440 h of stability for CNT-decane nanofluid using oleylamine as stabilizer. Several studies on carbon based nanofluid have been compiled in Table 1, which shows the use of stabilization techniques for enhancing the stability of nanofluid.

2.4. Hybrid/mixed metal based nanofluid

Hybrid nanofluid is a relatively new breed of nanofluid where more than one type of nanoparticle is combined in a nanofluid resulting in superior thermal properties compared to nanofluids made of single type of nanoparticles. Nine et al. [17] prepared Al_2O_3–MWCNT-Water nanofluid and observed 8% increment in thermal conductivity value compared to pure Al_2O_3 nanofluid. Several studies have used different types of hybrid nanofluid such as Ag-MWCNT [18], MWCNT-Fe_3O_4 [19], Nanodiamond-Fe_3O_4 [20] etc. for lubrication, heat transfer (thermal conductivity) and electrical conductivity enhancement applications respectively. Layered double hydroxide nanofluid is a type of hybrid nanofluid which combines two or three metal ions (both bivalent and trivalent metal ion) together into a single nanoparticle. Chakraborty et al. [21] prepared Cu-Al LDH-water nanofluid using co-precipitation technique and reported 16.1% increment in thermal conductivity value for 0.8 vol% nanofluid. Summary of different studies focused on stability and preparation method of hybrid nanofluid has been reported in Table 1. Both one-step and two-step method are used for preparation of hybrid based nanofluid. Overview of different nanofluid preparation methods are discussed in the following section.

3. Nanofluid preparation method

Nanofluids are generally synthesized using two basic methods i.e. (a) one-step method, and (b) two-step method. Table 1 summarizes methods of nanofluid preparation for different types of nanofluids. A brief summary on both the synthesis schemes is presented in the following sections.

3.1. One step method

The one-step synthesis method refers to the preparation of nanofluid directly in basefluid without the need of several intermediate steps such as particle drying, storage, and dispersion of nanoparticle in the basefluid [38]. The one-step synthesis scheme enables simultaneous synthesis and dispersion of nanoparticle in the basefluid. The stability of nanofluid prepared using this technique is mostly superior compared to the two-step method. This methodology eliminates the chances of particle agglomeration during the drying process. Akoh et al. [39] synthesized oil based ferromagnetic (Fe, Ni, and Co) nanofluid using direct evaporation technique, which is commonly known as VEROS (Vacuum Evaporation on Running Oil Substrate). Lo et al. [40] prepared copper oxide, copper dioxide and copper nanoparticle in dielectric liquids as basefluid (deionized water, ethylene glycol (EG) and mixture of water-EG) using SANSS (Submerged Arc Nanoparticle Synthesis System). This method allows excellent control over the nanoparticle shape (needle like, polygon shaped, square and circular shaped) with minimal agglomeration of the nanoparticle. TEM analysis revealed the formation of nanoparticle having different shape and uniform size distribution. Selection of dielectric liquid plays a critical role in determining the shape of nanoparticle.

In general, one-step method is impractical for large scale nanofluid synthesis due to its high production cost. Therefore, relatively low-cost one-step chemical process has garnered immense attention among the nanofluid fraternity. Zhu et al. [41] synthesized Cu-EG nanofluid by reducing copper sulphate and sodium hypophosphite monohydrate in a medium of ethylene glycol (EG) using microwave irradiation. Polyvinylpyrrolidone (PVP-K30) was used as a stabilizer. This method produced uniformly distributed Cu nanofluid with excellent stability. The nanofluid stability was tested at elevated temperature under stationary condition for 14 days during which it showed no sign of sedimentation. The enhanced stability of synthesized nanofluid is attributed to three factors, (a) lower particle size, (b) better dispersibility in basefluid, and (c) addition of PVP as a steric stabilizer. Similarly, microwave irradiation of $AgNO_3$ and PVP in ethanol medium was performed to form stable silver nanofluid [42]. Silver nanofluid prepared using this method remained stable for a duration of 30 days under stationary condition at room temperature and over a duration of 10 h without any sedimentation under the influence of centrifugal force (at 3000 rpm). Yu et al. [43] reported synthesis of stable homogeneous n-octane based graphene oxide (GO) nanofluid using phase transfer method. Graphene oxide nanoparticles are typically hydrophilic in nature and can be easily suspended in water due to the presence of oxygen containing functional groups such as −COOH (carboxylic), −OH (hydroxyl), and −C═O (carbonyl). In order to make GO compatible with organic solvents, oleylamine was used as a modifier to convert graphene oxide nanoparticle to hydrophobic nanoparticle which enable its dispersion in organic solvent. Ayyappan et al. [44] reported one-step synthesis techniques of different metal based nanofluid (Ag, Au, Cu and Pd) in ethanol medium using PVP as stabilizer.

In a nutshell, it can be concluded that one step nanofluid synthesis method involves insitu preparation and dispersion of nanoparticle in basefluid in a single step (VEROS, SANSS, microwave irradiation, phase transfer etc.) without the need of intermediate particle drying step.

Key advantages are as follows:

1. Synthesis of nanoparticle and its dispersion in basefluid is performed simultaneously.
2. Storage, drying and transportation of particle are avoided which limits the probability of particle aggregation.
3. Stable nanofluid can be prepared without any additional stabilizer.

4. There is greater control over nanoparticle size and shape during synthesis process.
5. Nanofluid is more stable in nature compared to two-step method.

Key disadvantages are as follows:

1. Nanofluid can only be prepared in batch wise manner and in low quantity.
2. In general, the synthesis method is expensive in nature.
3. The unreacted reactants remaining in end product can create problem during application.

3.2. Two step method

Two-Step synthesis of nanofluid is the most commonly used method of nanofluid preparation. This method is cost effective and can be easily implemented. The main drawback of this technique is the control of particle agglomeration tendency. The frequent implementation of extensive ultrasonication and stirring is the most commonly used method to control agglomeration. Addition of different surfactants such as:

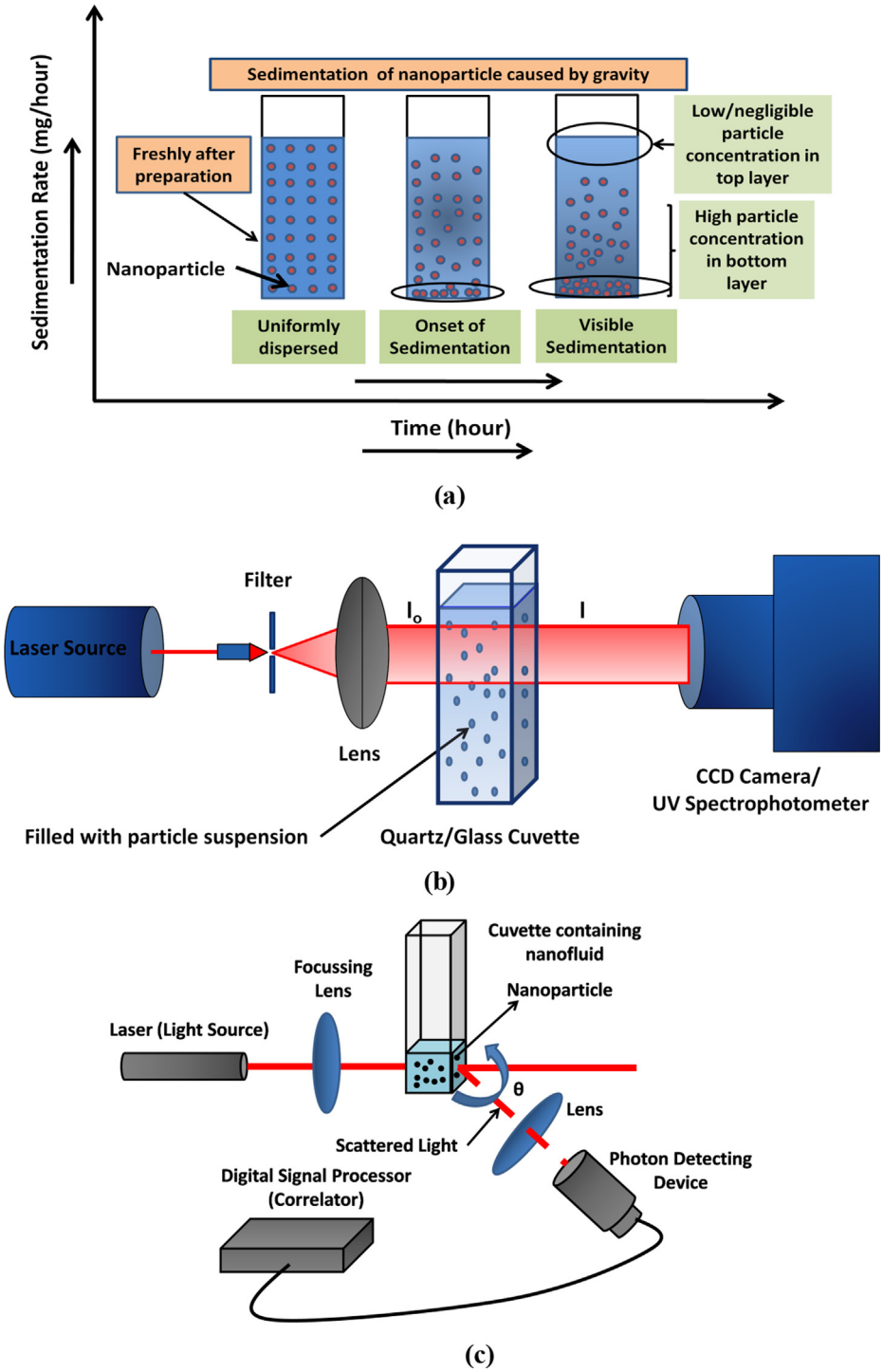

Fig. 1. Schematic of different nanofluid stability estimation techniques; (a) sedimentation measurement, (b) transmittance/absorbance measurement, and (c) dynamic light scattering measurement.

Anionic (Sodium Dodecyl Sulphate (SDS), Sodium Dodecyl Benzene Sulphonate (SDBS)), *Cationic* (Cetyltrimethylammonium Bromide (CTAB)), *Non-ionic* (Span 80, Tween 20) and *polymer* (Polyvinyl Pyrrolidone (PVP), Poly Vinyl Alcohol (PVA), Gum Arabic (GA)) during nanofluid preparation is another method of controlling particle aggregation [3,32,37,45–47]. Several researchers have also used two-step method to prepare stable nanofluids without using any surfactants or polymer [24,48].

In brief, it can be concluded that two-step nanofluid synthesis method involves two distinctive stages of preparation; a) preparation and drying of nanoparticle, and b) dispersion of nanoparticle in basefluid using physical (ultrasonication, magnetic stirrer, and high pressure homogenizer) and chemical (electrostatic, steric and electrosteric) methods.

Key advantages are as follows:

1. Two-step method is ideal for large scale and cost-effective production.

Key disadvantages are as follows:

1. Nanoparticles prepared by this method are more prone to agglomeration.
2. Frequent application of ultrasonication, homogenization or stabilizer addition is needed to stabilize the nanofluid for longer duration.
3. There is limited control over particle size and shape during synthesis. Nanoparticles also tend to agglomerate during storage or drying period.

4. Stability evaluation methods

Several techniques are used in literature for the evaluation of nanofluids stability i.e. (a) sedimentation and centrifugation, (b) zeta potential measurement, (c) spectral absorbance and transmittance measurement, (d) 3 ω method, (e) transmission electron microscopy, and (f) dynamic light scattering. A brief description of these techniques is provided in the following section.

4.1. Sedimentation and centrifugation

Sedimentation is the most commonly used technique for stability evaluation. This technique is based on formation of sediment at the bottom of the liquid column due to gravity. The longer time taken by the nanofluid for formation of precipitate is an indication of superior stability of nanofluid. Several researchers have used the sedimentation technique to evaluate nanofluid stability [1,32,36]. Centrifugation technique is an alternative sedimentation technique which requires relatively lower time to evaluate the nanofluid stability. In this method, the centrifugal force is much stronger than the normal gravitational force which accelerates the sedimentation process. Singh et al. [42] prepared ethanol based Ag nanofluid with PVP as stabilizer and examined its stability using the centrifugation techniques at 3000 rpm for 10 h. The nanofluid displayed no sign of sedimentation within the aforementioned time frame which is comparable to what was observed by conventional sedimentation techniques for 1 month.

Fig. 1(a) schematically illustrates the sedimentation based stability evaluation method. The terminal settling velocity (V_t) for a spherical, smooth nanoparticle in a centrifuge can be determined considering stokes law regime ($Re_p < 1$) using the following expression [49],

$$V_t = \frac{D_p^2(\rho_p - \rho_o)\omega^2 X}{18\mu} \quad (1)$$

where D_p, X, ρ_p, ρ_o, ω and μ represents particle diameter, distance between axis of rotation and specific location of the tube inside centrifuge, density of nanoparticle, density of base fluid, angular velocity of centrifuge and viscosity of basefluid, respectively. This equation clearly indicates that low particle size, higher viscosity of basefluid and nominal density difference between nanoparticle and basefluid are key to achieving higher nanofluid stability. It is also to be pointed out that lowering particle size increases surface energy which in turn can lead to particle clustering. Higher settling velocity indicates faster settling of nanoparticle. Both sedimentation and centrifugation technique provide quantitative evaluation of stability in terms of settling time or by measuring the height of sediment layer with respect to time.

4.2. Zeta potential measurement

Zeta potential is used as a measure of nanofluids stability and more details on the criteria of stability based on zeta potential have seen presented in a later section. Colloidal suspension with high zeta potential value is stable in nature and suspension having lower zeta potential value tends to agglomerate faster and is considered unstable. Several researchers have used zeta potential measurement as the tool to quantify the stability of nanofluid. Table 1 presents the stability of different types of nanofluid based on zeta potential measurement.

4.3. Spectral absorbance and transmittance measurement

Spectral absorbance and transmittance measurement can provide a quantitative measure of nanofluid stability. This method of stability evaluation is generally used when the nanoparticle suspended in the basefluid has an absorption peak between 190 and 1100 nm [50]. The particle suspended in the base fluid has tendency to absorb light in the visible and ultraviolet frequency range. Stability is measured by constantly checking the absorption peak characteristics using UV–VIS spectrophotometer and how it varies with time. Decrease in absorbance with time indicates instability of nanofluid suspension. Absorbance (A_λ) is proportional to concentration of particle in the solution given as,

$$A_\lambda = \log_{10}(I_o/I) = \alpha \times l \times c \quad (2)$$

where I, I_o, α, l and c, represent intensity of laser light beam after passing through the colloidal suspension, intensity of incident laser light, absorptivity, length of light path and concentration of particle respectively. The decrease in nanoparticle concentration with time due to sedimentation is reflected in decrease of absorbance value. However, for nanofluid with dark coloured nanoparticle and high particle concentration, it is difficult to measure the stability using this method [51,52].

Similarly, transmittance measurement can also be used for stability evaluation. Transmittance (T_λ) and absorbance (A_λ) are related to each other as:

$$T_\lambda = I/I_o \quad (3)$$

Measurement of transmittance at different time intervals can provide measure of nanofluid stability. Fig. 1(b) shows a schematic of experimental arrangement for transmission or absorbance measurement. He-Ni laser is used as the light source having a wavelength of 632 nm. CCD camera or UV spectrophotometer is used to capture the image intensity at specific wavelength. Increase in transmittance with time is an indication of nanofluid instability. A sample stability measurement data of Cu-Al LDH nanofluid has been shown in Table 2. The table shows increase in transmittance value with increasing time as a function of initial nanoparticle concentration. The nanofluid shows greater instability at higher concentration of nanofluid.

4.4. 3 ω method

The 3 ω method of stability analysis uses change in thermal conductivity of nanofluid due to particle agglomeration and sedimentation as a measure of instability [53]. This method can be implemented for

Table 2
A sample stability measurement results of Cu-Al LDH nanofluid at different particle concentration and time interval using transmittance measurement.

Sample	Concentration (vol%)	%Transmittance		
		Day 0	Day 2	Day 3
Water	0	100	100	100
Cu-Al LDH nanofluid	1	77.21	81.70	85.22
	2	72.78	77.78	81.72
	4	30.03	36.34	42.34

nanofluid having a wide range of volume fraction. Oh et al. [54] reported increase in thermal conductivity of Al_2O_3-water and Al_2O_3-EG nanofluid with time (up to 1 h) and concluded that such an increment in thermal conductivity is a result of particle clustering/agglomeration. There exists an optimum degree of particle clustering beyond which further agglomeration leads to decline in thermal conductivity [55]. Karthikeyan et al. [56] observed 22.5% decrease in thermal conductivity of CuO-water nanofluid with time (within a time interval of 20 min) due to agglomeration and subsequent sedimentation of nanoparticles. Decline in thermal conductivity of nanofluid is attributed to particle clustering which reduces surface area to volume ratio and effective thermal interaction area.

4.5. Transmission electron microscopy

Transmission Electron Microscopy (TEM) can be used to observe particle agglomeration of nanofluid and the particle size distribution measurement can be used as an alternative measure of nanofluid stability. High resolution TEM image provides two dimensional image of nanoparticle suspended in the basefluid. Several researchers have used this technique to comment on the extent of particle aggregation, particle size and shape of different nanofluids [32,36,37,53]. Chakraborty et al. [32,37] reported the effect of surfactant and polymer addition on the dispersion of TiO_2 and Cu-Zn-Al LDH nanoparticle in aqueous medium and reported the stability results based on TEM measurement, which correlate well with zeta potential and sedimentation measurements.

4.6. Dynamic light scattering

Dynamic light scattering (DLS) technique can be used to measure the particle size distribution of any colloidal suspension. Fig. 1(c) shows key components of a DLS measurement setup. A laser is used to illuminate suspended nanoparticle in the basefluid. A photon detector monitors the scattered light fluctuation caused by the particle Brownian motion. The diffusion coefficient is calculated from intensity fluctuation using light scattering theory. The measured diffusion coefficient is used to calculate the particle size using Stokes-Einstein equation [57] as:

$$R_H = \frac{k_B T}{6\pi\mu D} \tag{4}$$

where R_H, D, k_B, T, and μ represent hydrodynamic radius, translational diffusion coefficient, Boltzmann constant, absolute temperature and viscosity respectively. Measurement of particle size acquired at different time intervals over a long period of time indicates the nanoparticle agglomeration tendency. The instability of nanofluid leads to formation of cluster which eventually leads to sedimentation. Therefore, DLS analysis can show increase in particle size with time due to agglomeration and act as indicator of nanofluid instability. Kole et al. [58] observed 9 times increase in cluster size of CuO nanoparticle in gear oil (basefluid) compared to its primary particle size due to instability of nanofluid. Sadeghi et al. [59] reported increase in cluster size of Al_2O_3–water nanofluid with time which is an indication of gradual aggregation of nanoparticle.

Table 3
Van der Waal attractive interaction potential for different particle shapes and configuration under different boundary conditions [60].

Geometry	Attractive Interaction Potential (V_A or V_{VdW})	Size Range
A = Hamekar constant (J), S = Particle separation distance (nm), a_1 = a_2 = a = Characteristic radius (nm), L = Length of cylinder (nm), A_{plate} = Area of interacting plate (m^2)		
Sphere/sphere	$V_{VdW} = V_A = -\frac{A}{6S} \times \left[\frac{a_1 a_2}{a_1 + a_2}\right]$ (6)	$a_1, a_2 \gg S$
Sphere/sphere	$V_A = -\frac{16 A a_1^3 a_2^3}{9S^6}$ (7)	$a_1, a_2 \ll S$
Plate/plate (semi-infinite)	$V_A = -\frac{A}{12\pi S^2} \times A_{plates}$ (8)	NA
Cylinder/cylinder (Parallel)	$V_A = -\frac{A}{12\sqrt{2}S^{3/2}}\left[\frac{a_1 a_2}{a_1 + a_2}\right] \times L$ (9)	$a_1, a_2 \gg S$
Cylinder/cylinder (Parallel)	$V_A \propto -\frac{1}{S^5} \times L$ (10)	$a_1, a_2 \ll S$
Cylinder/cylinder (crossed)	$V_A = -\frac{A\sqrt{a_1 a_2}}{6S}$ (11)	$a_1, a_2 \gg S$
Plate/sphere	$V_A = \frac{-Aa}{6S}\left(1 + \frac{S}{2a+S} + \frac{S}{a} ln\left(\frac{S}{2a+S}\right)\right)$ (12)	$a \gg S$
Plate/sphere	$V_A \propto -\frac{1}{S^3}$ (13)	$a \ll S$

5. Stability mechanism

Stability of colloidal suspension can be explained using a theory proposed by Derjaguin, Landau, Vewey, and Overbeek (DLVO). This theory is based on the following assumptions: (1) particle dispersion is dilute, (2) Van der Waal attractive force and electrostatic force are the only two forces acting on the suspended particle, (3) gravity and buoyancy forces are neglected, (4) the colloidal suspension is homogeneous in nature and (5) ion distribution throughout the colloidal system is dependent on three factors namely, electrostatic force, Brownian motion and entropy induced dispersion.

According to the DLVO theory, colloidal stability is dependent on the total potential energy, V_T which is expressed as:

$$V_T = V_A + V_R \tag{5}$$

where V_A and V_R represent Van der Waal attractive potential and electrostatic repulsive potential respectively. The expressions of Van der Waal attractive potential and electrostatic repulsive potential for particles of different size and shape have been compiled in Tables 3 and 4 respectively. Fig. 2 schematically depicts different configuration of particles with size (a_1, a_2), shape (spherical, cylindrical, plate) and separation distance (S).

From the expression of Van der Waal attractive potential (V_A), the importance of Hamekar constant is quite evident. Hamaker constant (A) is dependent on refractive index of material used and dielectric property of the basefluid which is expressed as:

$$A = (A_1^{\frac{1}{2}} - A_2^{\frac{1}{2}})^2 \tag{21}$$

where A_1 and A_2 are the Hamekar constants of the particle and medium respectively. The value of Hamekar constant for silver (Ag)-water, Ag-methanol, alumina(Al_2O_3)-water and Al_2O_3-methanol nanofluid system are 149.1 × 10^{-21} J, 175.2 × 10^{-21} J, 36.9 × 10^{-21} J and 84.4 × 10^{-21} J, respectively [61]. Particles having high Hamekar constant are more prone to agglomeration due to high Van der Waal attractive potential [62,63].

For ease of electrostatic repulsive interaction potential calculation, the surface potential (φ) is assumed as zeta potential (ζ) value. Eq. 15 is valid when κa < 5 which is common in case of nanoparticles. Debye constant (κ) is expressed as [62],

$$\kappa = \sqrt{\frac{n\sum_i (Z_i e)^2}{\varepsilon k_B T}} \tag{22}$$

Table 4
Electrostatic repulsive interaction potential (Derjaguin approximation) for different particle shapes and configuration under different boundary conditions [60].

Geometry	Repulsive Interaction Potential (V_R or V_{ES})	Size and Potential Range
S = Particle separation distance (nm) , $a_1 = a_2 = a$ = Characteristic radius (nm), a_s = Radius of sphere, a-c = Radius of cylinder L = Length of cylinder (nm), φ = Surface potential (mV), ε = Dielectric constant of basefluid, εo = Permittivity of vacuum (F/m) and κ^{-1} = Debye length (nm)		
Sphere/sphere $a = a_1 = a_2$ $\varphi = \varphi_1 = \varphi_2$	$V_R = 2\pi\varepsilon\varepsilon_0 a\varphi^2 ln(1 + exp(-\kappa S))$ (14) Boundary Condition: Constant Potential	κa ≫ 1 φ ≤ 25 mV
Sphere/sphere $a = a_1 = a_2$	$V_R = 2\pi\varepsilon\varepsilon_0 a\varphi^2 exp(-\kappa S)$ (15) Boundary Condition: Constant Potential	κa < 5 φ ≤ 25 mV
Plate/plate $\varphi = \varphi_1 = \varphi_2$	$V_{R,plates} = \varepsilon\varepsilon_O \kappa\varphi^2\left(1 - tanh\left(-\frac{\kappa S}{2}\right)\right)$ (16) Boundary Condition: Constant potential	φ ≤ 25 mV
Cylinder/cylinder (Parallel) $a_1 \neq a_2$	$V_R = \sqrt{\frac{2a_1a_2}{a_1+a_2}}\left(\int_S^\infty \frac{V_{R,plates}}{\sqrt{(x-S)}}dx\right) \times L$ (17)Boundary Condition: Constant Potential	Use Eq. 16 for $V_{R,plates}$ κa ≫1; a > S
Cylinder/cylinder (Crossed)	$V_R = 2\pi\sqrt{a_1a_2}\int_S^\infty V_{R,plates}dx$ (18)Boundary Condition: Constant Potential	Use Eq. 16 for $V_{R,plates}$ κa ≫1; a > S
Cylinder/sphere	$V_R = \frac{2\pi a_s\sqrt{a_c}}{\sqrt{a_s+a_c}}\int_S^\infty V_{R,plates}dx$ (19)Boundary Condition: Constant Potential	Use Eq. 16 for $V_{R,plates}$ κa ≫1; a > S
Plate/sphere	$V_R = 2\pi a\int_S^\infty V_{R,plates}dx$ (20)Boundary Condition: Constant Potential	Use Eq. 16 for $V_{R,plates}$ κa ≫1; a > S

where e, n, Z_i, k_B, and T denotes single electron charge, number density of ionic species in the solution, ions valency, Boltzmann constant (1.3806×10^{-23} $J.K^{-1}$), and temperature respectively. The inverse of Debye constant is known as Debye length (nm).

The stability of the colloidal suspension depends on the sum of V_A and V_R, which is a function of separation distance between the particles. The two nanoparticles approach towards each other due to Brownian motion changing the separation distance and interaction potential. If V_A dominates over V_R, then nanoparticles would tend to form a large cluster and destabilize the suspension. Fig. 3 shows the variation of potential energy with respect to separation distance for two situations: (1) when total interaction potential is low, particle would tend to settle faster (See Fig. 3(a)) and (2) when total interaction potential is high, particle prevents agglomeration and remains stable. However, despite having sufficient energy barrier, if two particles collide with sufficient energy i.e. at elevated temperature, it can overcome the aforesaid barrier. Once the barrier is breached, attractive force will dominate over the repulsive force and pull the two particles together to form cluster. These clusters are irreversible in nature and get strongly attached. When the zeta potential value of the suspension is low and particle loading is high, Van der Waal potential can dominate over repulsive potential (particle separation distance is low) which creates a secondary minimum (See Fig. 3(a)). Due to this secondary minimum, weakly bonded clusters can be created. These clusters can be broken up by external forces using vigorous agitation and ultrasonication to form stable nanofluid suspension. When particles have sufficiently high repulsive force, there is less agglomeration. Without a strong repulsive potential, flocculation and coagulation can take place which is undesired. Therefore, to ensure long term stability of the nanofluid, it is essential to have high repulsive potential. The effect of a high potential barrier on nanofluid stability is shown Fig. 3(b).

6. Factors responsible for nanofluid stability

Different parameters i.e. dielectric constant and pH value of basefluid, zeta potential, size and shape of particle, and particle concentration affect the stability of nanofluid. The mechanism explaining the influence of these factors on nanofluid stability is discussed in the following sections.

6.1. Dielectric constant of basefluid

The dielectric constant of the basefluid is directly proportional to the repulsive potential which means higher the dielectric constant greater will be the stability (See Table 4). The dielectric constant of conventional basefluid such as acetone, ethanol, ethylene glycol, hexane, benzene, and water are 21.01, 24.6, 24.6, 1.89, 2.28 and 78.5, respectively at 20 °C [64]. The highest dielectric constant is observed for water among other basefluid which indicates its high repulsive potential.

6.2. Zeta potential

When nanoparticles are suspended in the base fluid, the liquid layer surrounding the particle can be divided into two parts; (a) stern layer, and (b) diffuse layer. In stern layer, ions are strongly attached with the particle whereas in diffuse layer, ions are loosely bounded. The amalgamation of surface charge, stern layer, and diffuse layer is known as electrical double layer (EDL) which consists of both positively and negatively charged ions but is electrically neutral. The zeta potential value provides a good estimation on the stability of nanofluid. High zeta potential value (both positive and negative) of suspension implies a higher repulsive force which prevents particles to come close to each other resulting in formation of aggregates. Particles having a zeta potential value greater than ± 30 mV are considered stable. Particles having zeta potential value in the range of ± 15 mV are considered unstable. Fig. 4(b) shows the interpretation of different zeta potential range on the nanofluid stability. It may be noted that if particle and base fluid has significant density difference, sedimentation can take place in spite of having high zeta potential value.

6.3. pH value

The pH value of the suspension and zeta potential value are correlated with each other. The effect of pH on the zeta potential value (stability) has been reported by several researchers [47,53,65,66]. The pH value affects the electrical charge density on the nanoparticle surface which in turn influences the stability of nanofluid. Fig. 4(a) shows the variation of pH value corresponding to zeta potential for different nanoparticles. Fig. 4(b) shows the schematic of different stability regime corresponding to zeta potential and pH values. At the isoelectric point (IEP), individual particles carry no net electric charge, and zeta potential value approaches zero. Nanofluid suspension near its IEP is considered to be unstable [67]. The pH value also affects the size and shape of nanoparticle during its preparation which influences the stability of the nanofluid. Li et al. [5] studied the effect of pH value on size and shape of synthesized Ag nanoparticle. In a basic medium (pH = 11), morphology of the Ag nanoparticles are spherical in nature

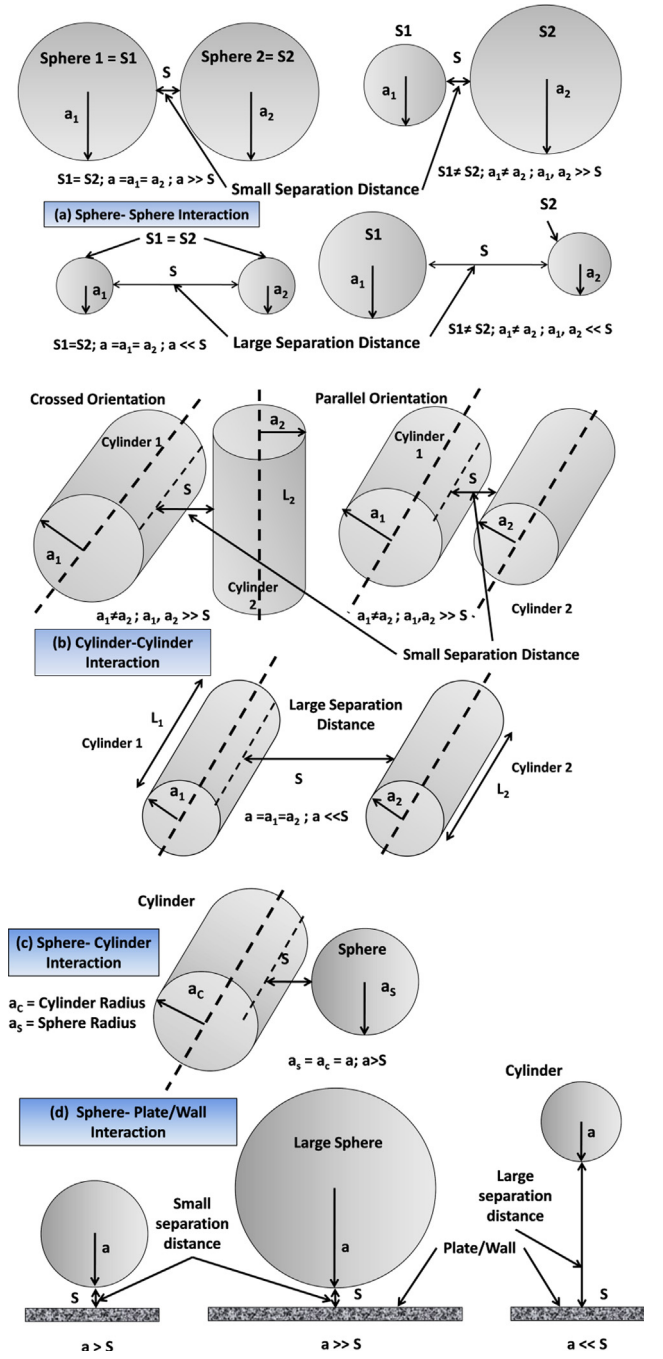

Fig. 2. (a–d). Schematic representation of nanoparticles with different size, shape (cylinder, sphere, plate), and orientation for calculation of interaction potential (See Tables 3 and 4).

and size distribution is uniform whereas in neutral medium, synthesized Ag nanoparticles vary in shape from nanosphere to nanorod and there is no control over size distribution. Fig. 5 shows the size distribution of nanoparticles based on TEM measurement. The effect of particle size and shape on nanofluid stability has been discussed in the following section.

6.4. Particle size and shape

Both Van der Waal attractive force and electrical double layer repulsive force are dependent on the particle size. When particle size is low, higher number of atoms are present on the particle surface [62] which results in increase in active site density. He et al. [68] observed that for hematite (α-Fe_2O_3) particles the tendency of aggregation is enhanced with decrease in particle size. For same pH and ionic strength, aggregation is higher for smaller particle size. The critical coagulation concentration and isoelectric point (pH value) decrease with decrease in particle size. Therefore, the agglomeration regime shifts towards lower pH value. Eqs. 14 and 15 in Table 4 reports two different expressions for repulsive interaction potential at $\kappa a \gg 1$ and $\kappa a < 5$. Walker et al. [60] reported mathematical expression for Van der Waal attractive and electrostatic repulsive potential for nanoparticle having different shape and orientation. Tables 3 and 4 summarize the effect of particle shape and particle orientation on the Van der Waal attractive and electrostatic repulsive potential under different condition [36]. Fig. 2 shows different geometrical configuration of nanoparticle having different shapes such as sphere-sphere, sphere-cylinder, sphere-plate and cylinder-cylinder interaction.

Calculation of attractive, repulsive and total interaction potential for hematite is carried out using equations shown in Tables 3 and 4 for $\kappa a < 5$ and Hamekar constant $A = 2 \times 10^{-20}$ J [68]. The zeta potential corresponding to different particle size is: ζ (d = 12 nm) = 42.6 mV, ζ (d = 32 nm) = 40.2 mV and ζ (d = 65 nm) = 44.1 mV. Fig. 6 demonstrates the effect of particle size (particle diameter, d = 12, 32 and 65 nm) on attractive, repulsive and total interaction potential of hematite (α-Fe_2O_3) nanoparticle as a function of separation distance. The figure clearly shows that with increasing particle size, repulsive (V_R) and total interaction potential (V_T) increases whereas attractive potential (V_A) decreases marginally.

Kim et al. [69] reported that the stability of water based bohemite alumina nanofluid is strongly dependent on the particle shape. According to their findings, stability of water based alumina nanofluid degrades with time differently depending on the shape of the particle. The blade shaped particles sediment faster than platelet and brick shaped particles. Brick shaped nanoparticles display a highly stable nature in the suspended form. The results obtained by the stability analysis is also theoretically validated by calculating interaction potential of nanoparticle having three different shapes (brick, blade and platelet) using equations in Tables 3 and 4. The effect of particle shape is not evident on attractive interaction potential, which varies only as a function of nanoparticle concentration. However, in case of repulsive potential, the shape effect is quite evident. Highest repulsive potential is reported in case of brick shaped particles and lowest is observed in case of blade shaped particle. High repulsive potential calculated using Eq. 15 (brick shaped nanoparticle) indicates high nanofluid stability which exactly matches with the experimental results on nanofluid stability.

Classical DLVO theory is valid only for spherical particles. When particles are in form of triangles, ellipses, rhombohedrons, spindle, platelets, and rod shape [62,63], it further complicates DLVO theory and affects both Van der Waal attractive force and electrostatic repulsive potential [70] prediction. According to Vold et al. [71], for a separation distance lower than the average particle diameter (anisometric particle), attraction force is more dominant than repulsive force because more atoms are available for interaction. The aggregate formation is more likely in case of anisometric nanoparticles than spherical ones. In case of cylindrical particles, parallel orientation is favoured over perpendicular orientation in terms of interaction potential. High aspect ratio nanoparticles are more prone to agglomeration. The settling velocity (V_t) of the nanoparticle in the basefluid is expressed by Stokes law [72]. Determination of settling velocity is dependent on the shape of particle as it directly affects the value of drag coefficient during settling process. Low particle size and nominal density difference between nanoparticle and basefluid lead to lower settling velocity and therefore superior nanofluid stability.

6.5. Particle concentration

The average particle separation distance reduces with increase in particle concentration. The lower separation distance implies greater

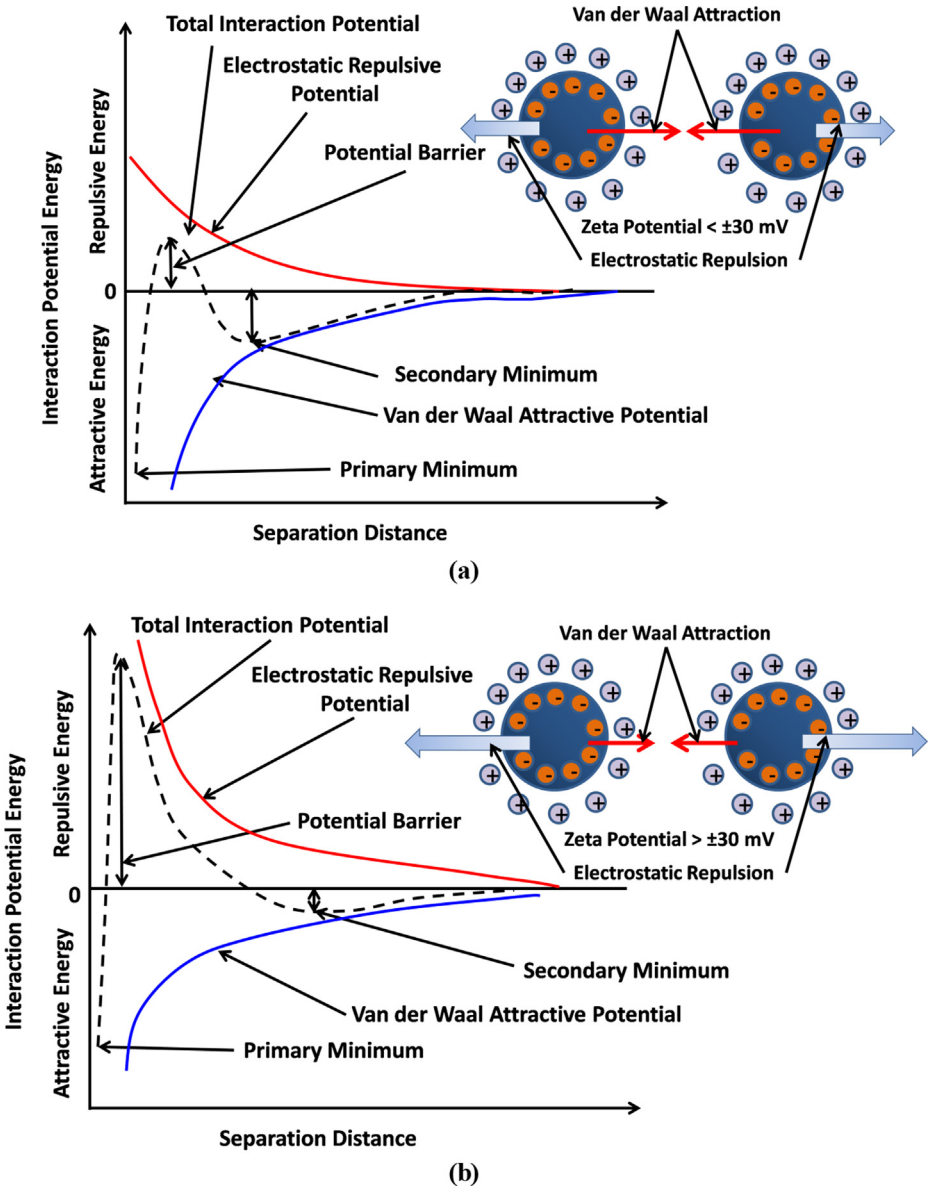

Fig. 3. Schematic diagram of interaction potential energy as a function of separation distance between nanoparticles for two situations: (a) when potential barrier is low, and (b) when potential barrier is high.

Van der Waal attractive potential (See Tables 3 and 4). When Van der Waal attractive potential dominates over electrostatic repulsive potential, particle agglomeration takes place. Therefore, effect of particle concentration plays a crucial role in determining nanofluid stability. Several researchers have reported poor stability of nanofluid at higher particle concentration [21,36]. Chakraborty et al. [36] observed that Cu-Zn-Al LDH nanofluid at 40 ppm of nanoparticle concentration remains stable whereas 240 ppm nanofluid suspension shows sign of sedimentation. Increase in particle concentration augments particle cluster size due to lower interparticle distance and enhanced Van der Waal attractive force which directly affects the settling velocity. Hong et al. [73] reported increase in average cluster size of Fe-EG nanofluid (0.2 vol% loading) with time from 1.2 μm to 2.3 μm. There is higher clustering tendency of nanofluid with increase in nanoparticle concentration. Chakraborty et al. [21] observed increase in cluster size from 86 nm to 126 nm with increase in nanoparticle concentration.

7. Nanofluid stabilization technique

This section reports different stabilization techniques for enhancing the stability of nanofluid suspension. Fig. 7 presents the classification of different stabilization approaches, which are broadly classified into mechanical and chemical techniques. These techniques have been elaborated in the following section.

7.1. Mechanical stabilization

Several mechanical stabilization approaches are used for reducing the cluster size of nanoparticles i.e. ultrasonic vibration and ball milling etc. The overview of these approaches is presented in the following sections.

7.1.1. Ultrasonic vibration

Nanofluid stability can be controlled by ultrasonication. Ultrasonication leads to the production of stable nanofluid by breaking the nanoparticle cluster. Ultrasonic vibration can be implemented in two ways; a) indirect method (ultrasonic bath), and b) direct method (probe sonicator). Among these two techniques, probe sonicator provides superior outcome in terms of breaking the particle cluster and lowering average cluster size (See Fig. 8). Several researchers have

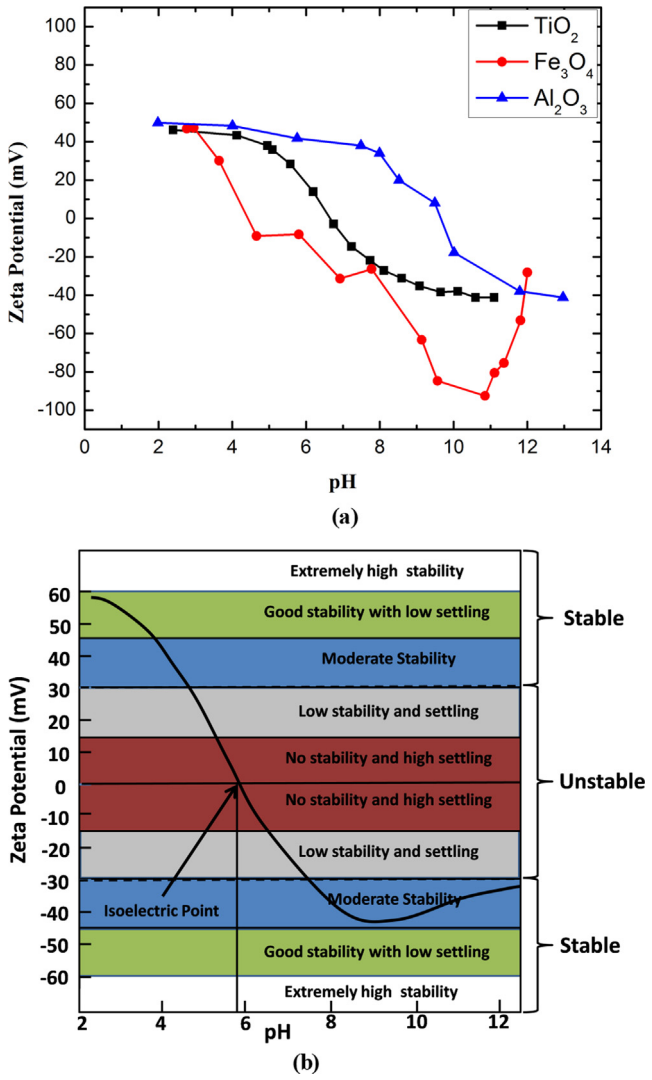

Fig. 4. (a) Zeta potential versus pH value of different types of nanofluid [53,65], and (b) schematic showing zeta potential and pH value corresponding to different regime of nanofluid stability.

reported the usefulness of ultrasonication in terms of stability, cluster size reduction and thermo-physical properties (thermal conductivity, viscosity) [74,75]. Sadeghi et al. [59] reported the stability of Al_2O_3 nanofluid using zeta potential and DLS (Dynamic Light Scattering) analysis. They reported that with increase in ultrasonic vibration time (0–180 min), zeta potential of nanofluid improves irrespective of nanoparticle concentration from 25 mV to 50 mV. The DLS measurement also showed decrease in nanoparticle cluster size with increase in ultrasonic vibration time. Nguyen et al. [76] reported the effectiveness of ultrasonication for producing monodisperse alumina nanofluid i.e. average nanoparticle cluster size reduced from 230 nm to 130 nm using 500 s of ultrasonication at 30% vibration amplitude.

Amrollahi et al. [77] studied the impact of ultrasonication on sedimentation and thermal conductivity of MWCNT/EG nanofluid and reported enhancement in stability and thermal conductivity. However, it may be noted that excessive ultrasonication in case of graphene or CNT based nanofluid can introduce defects in their structure and lead to shortening of CNT length. Therefore, optimized sonication is desirable to prevent such defects [78]. Sadri et al. [79] discussed thermo-physical aspect (thermal conductivity, viscosity and density) of ultrasonication. Ultrasonication is associated with increase in temperature of suspension which influences its thermo-physical properties. It is recommended to use ultrasonication in programmable pulse and auto turning mode to control the temperature rise while using nanofluid having heat sensitivity. Chen and Wen [80] reported that beyond an optimal ultrasonication time particle size remains unchanged.

7.1.2. Ball milling

Planetary ball milling technique is also used to prepare a stable nanofluid suspension. Munkhbayar et al. [18] prepared aqueous MWCNT nanofluid with combined use of planetary ball mill and ultrasonication technique. Planetary ball milling helps to lower down the average cluster size and increase in the stability of resultant nanofluid. Boopathy et al. [81] reported the synthesis (two-step method) of Al and Cu nanofluid using a combination of PBM (wet milling), ultrasonication, and magnetic stirring.

7.1.3. Other techniques

In addition to ultrasonic and ball milling techniques, other methods of mechanical mixing are also used for nanofluid preparation. Stirrer (Magnetic and Mechanical), shaker and vortex mixer are also used for preparation of stable homogeneous nanofluid [21,32]. Magnetic stirrer is an essential tool for nanofluid preparation. The optimization of magnetic stirring speed is essential to avoid bubble formation during the nanofluid preparation [82]. However, this technique cannot maintain nanofluid stability over long duration of time and in many cases are ineffective at higher particle loading. High shear homogenizer and high pressure homogenizers are considered as effective tools to improve nanofluid stability by breaking down the cluster into original particle size [53,83,84]. Fedele et al. [85] synthesized water based CuO, TiO_2, SWNT nanofluids using high pressure homogenization which showed promising results compared to ultrasonication (more reduction in cluster size). Drzazga et al. [86] prepared CuO-water nanofluids by a combination of non-ionic surfactant, ultrasonication, and high pressure homogenizer.

7.2. Chemical stabilization

The nature of nanoparticle (hydrophilic or hydrophobic) influences the choice of basefluid i.e. polar or non-polar. Hydrophilic nanoparticles such as metal oxides (Al_2O_3, TiO_2, CuO) and graphene oxide are easily dispersed in polar solvent such as water. Non-polar basefluids (oil) are preferred for hydrophobic nanoparticles (CNT, Graphene). Use of additional stabilizer is not required in these cases as stability can be improved by using ultrasonication and homogenization techniques. However, in order to form stable nanofluid by mixing hydrophilic nanoparticle in non polar solvent or vice versa different chemical based stabilization techniques are required. The chemical stabilization technique can be classified into three types: (a) electrostatic, (b) steric, and (c) electrosteric stabilization. The electrostatic stabilization of nanofluid can be achieved by three ways i.e. using ionic surfactant, pH adjustment, and covalent surface functionalization. Steric stabilization can be attained by non-ionic surfactant and polymer addition. To achieve combined effect of electrostatic and steric stabilization, ionic polymer or ionic liquids are used. An overview of these three chemical stabilization techniques is presented in the following section. Fig. 7 presents classification of different chemical stabilization methods. Table 5 provides a detailed summary on the implementation and performance of different chemical based nanofluid stabilization techniques for different types of nanofluid.

7.2.1. Electrostatic stabilization

Electrostatic stabilization of nanofluid can be achieved when Van der Waal attractive force is counter balanced by electrostatic repulsive force acting between two similarly charged particle (See Fig. 9(a)). Particles involved in electrostatic stabilization can possess surface charge either by ionization of surface groups or by adsorption of ionic surfactant on the surface. Nanoparticles acquire charge by adsorption of ions from the dispersing media. The charged nanoparticles then attract

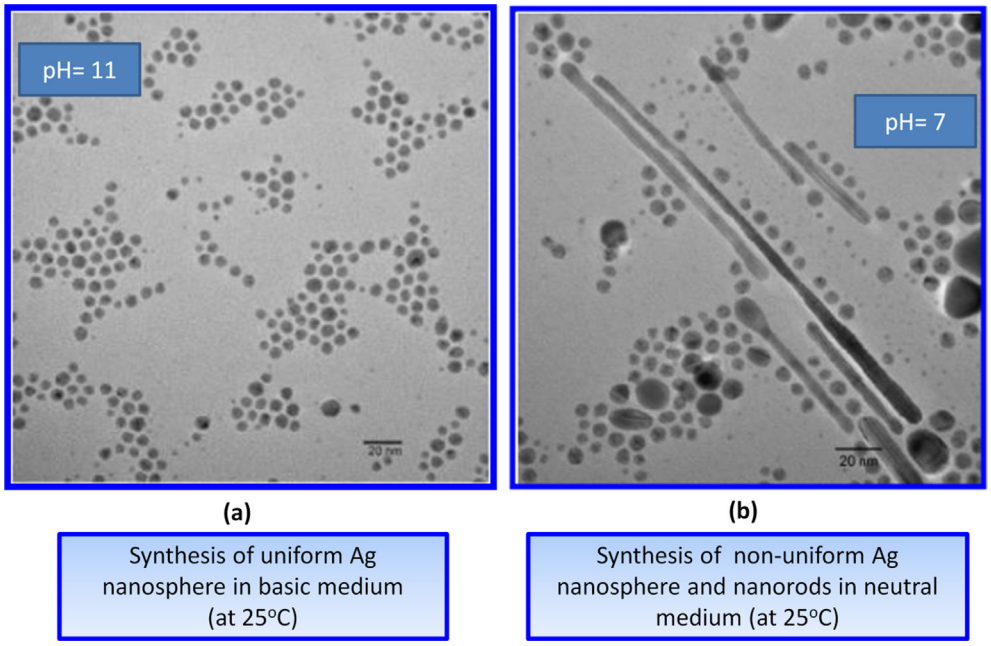

Fig. 5. TEM image showing the effect of pH value of dispersing medium on the size distribution and shape of Ag nanoparticle: (a) basic medium, and (b) neutral medium [5].

the counter ions which surround the particle surface. The electrical double layer is a layer of ions surrounding a particle dispersed in a base fluid. The electrostatic stabilization of nanoparticle is achieved by the overlapping of electrical double layer. Positive charge density surrounding the negatively charged particles provides electrostatic repulsion force which ensures nanoparticle dispersion in basefluid. The surroundings of nanoparticle can be divided into three distinctive zones: (a) surface charge is the region which consists of charges adsorbed by nanoparticle, (b) stern layer consists of the counter-ions which are strongly attached to the particle surface by electrostatic

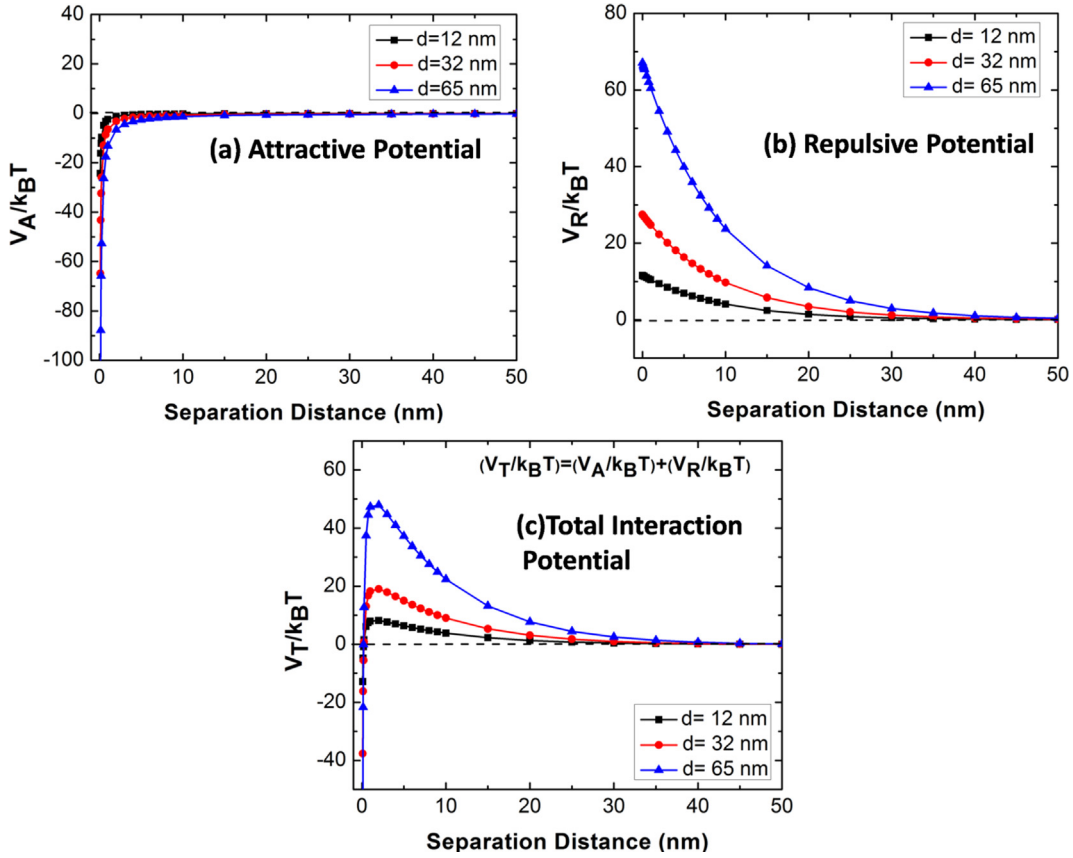

Fig. 6. Effect of particle size (d = 12, 32, and 65 nm) on (a) attractive (V_A), (b) repulsive (V_R), and (c) total interaction potential (V_T) between two spherical hematite (α-Fe_2O_3) nanoparticles as a function of particle separation distance.

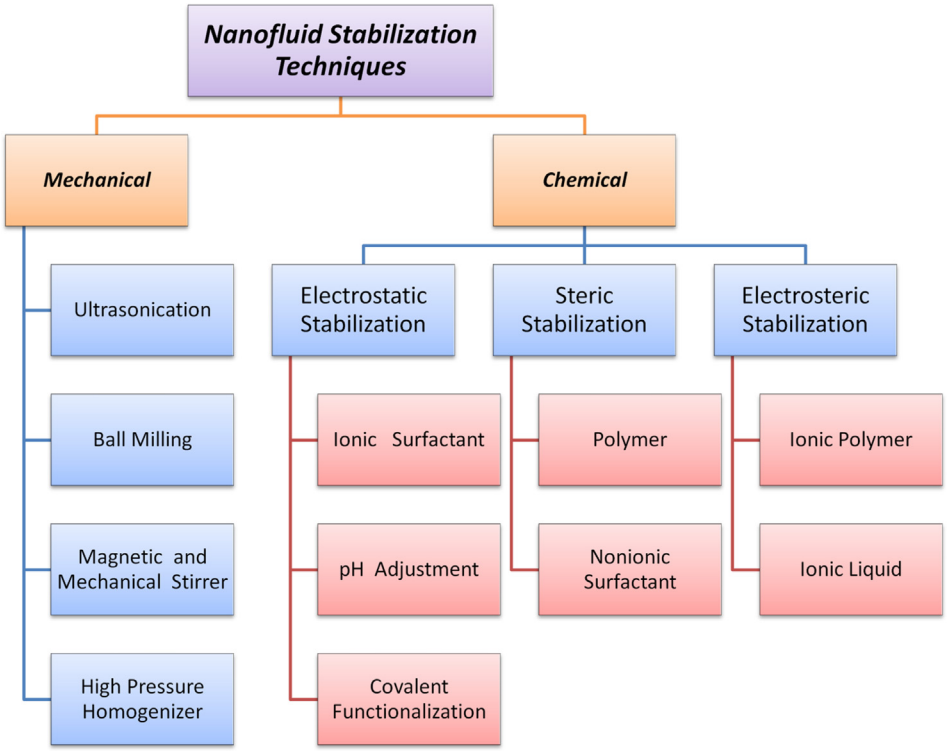

Fig. 7. Classification of nanofluid stabilization techniques.

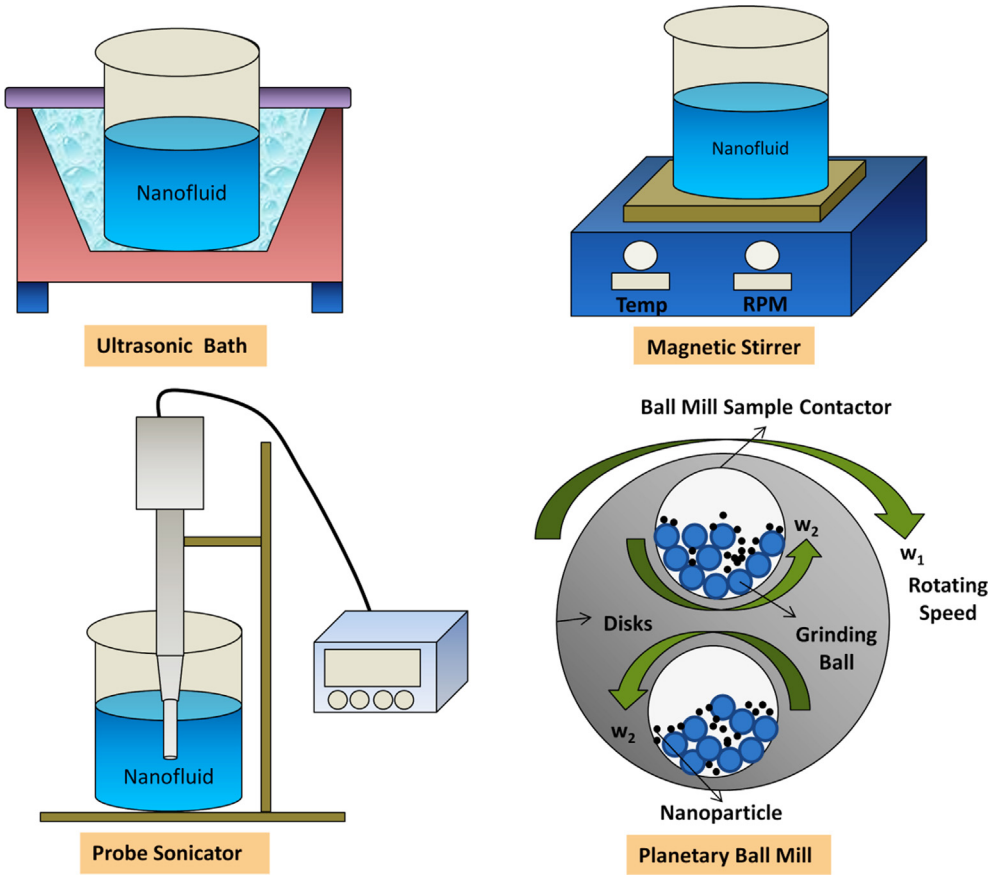

Fig. 8. Schematic of different types of equipment for nanofluid stabilization via mechanical route.

Table 5
Summary of implementation and performance of different nanofluid stabilization techniques.

Authors	Nanoparticle	Basefluid	Surfactants	Stability Duration and Zeta Potential	Stabilization Technique
Carbon based nanofluid					
Srinivas et al. [137]	CNT	Water	None	20.5 mV	None
	CNT	Carboxylated Water	Sebacic Acid, 2 Ethylexanoic Acid	38.2 mV	Electrostatic
Bandyopadhyaya et al. [128]	SWCNT	Water	GA	3 months	Steric
Wu et al. [138]	SWCNT	Water	Humic Acid	10 days	Electrostatic
Islam et al. [104]	SWCNT	Water	SDBS	3 months	Electrostatic
Tang et al. [131]	MWCNT	Water	PVP	2 months	Steric
Tang et al. [131]	MWCNT	Water	Triton X-100	2 months	Steric
Yu et al. [139]	MWCNT	Water	SDS	3 months	Electrostatic
Kim et al. [133]	MWCNT	Water	SDBS	1 day	Electrostatic
Kim et al. [133]	MWCNT	Water	CTAB	1 day	Electrostatic
Wusiman et al. [2]	MWCNT	Water	SDS	1 month	Electrostatic
Wusiman et al. [2]	MWCNT	Water	SDBS	1 month	Electrostatic
Fedele et al. [85]	Single Wall Cabon	Water	None	35 mV	None
	Nanohorn (SWCNH)	Water	SDS	15 days, −40 mV	Electrostatic
Hwang et al. [132]	Carbon Black	Water	SDS	−26.9 mV	Electrostatic
Metal based nanofluid					
Li et al. [140]	Cu	Water	CTAB	7 days, 28.1 mV	Electrostatic
	Cu	Water	SDBS	7 days, −43.8 mV	Electrostatic
	Cu	Water	Triton X-100	7 days, −8.3 mV	Steric
Wang et al. [47]	Cu	Water	SDBS	−43.8 mV	Electrostatic
Hwang et al. [132]	Ag	Silicon Oil	Oleic Acid	2 months	Steric
Li et al. [5]	Ag	n-heptane	Oleic Acid & N-Butylamine	1 month	Steric
Metal Oxide based nanofluid					
Sahooli et al. [129]	CuO	Water	PVP	7 days 32.3 mV	Steric
Sandhu et al. [141]	CuO	Water	SDS	2 days, 40 mV	Electrostatic
	CuO	Water-EG (50:50)	SDS	4 days, 47 mV	Electrostatic
	Al_2O_3	Water-EG (50:50)	None	28 days, 57 mV,	None
Choudhury et al. [142]	Al_2O_3	Water	None	14 mV	None
	Al_2O_3	Water	SDS	16 days −30 mV	Electrostatic
Wang et al. [47]	Al_2O_3	Water	SDBS	−40.1 mV	Electrostatic
Mo et al. [143]	TiO_2	Water	SDS	12 days	Electrostatic
Ghadimi et al. [144]	TiO_2	Water	None	2 days, −33.3 mV	None
	TiO_2	Water	SDS	7 days & −55 mV	Electrostatic
Bagaria et al. [145]	Fe_3O_4	Saline Water (NaCl, $CaCl_2$ in water)	Poly(2-acrylamido-3 methylpropanesulfonate-co- acrylic acid)	−45 mV	Electrosteric
Iqbal et al. [146]	Fe_3O_4	Saline Water (NaCl, $CaCl_2$ in water)	Poly(AMPS-co-AA)	1 month, −53.6 mV	Electrosteric
Hybrid nanofluid					
Song et al. [147]	Stainless steel	Water	SDBS	10 days, −70 mV	Electrostatic
Song et al. [147]	Stainless steel	Water	CTAB	10 days, 60.1 mV	Electrostatic
Chakraborty et al. [36]	Cu-Zn-Al LDH	Water	None	18 h, 38.6 mV	None
Chakraborty et al. [37]	Cu-Zn-Al LDH	Water	SDS	> 1 day, −50.6 mV	Electrostatic
	Cu-Zn-Al LDH	Water	Tween 20	12 h, 24.3 mV,	Steric

force, and (c) diffuse layer consists of both positively and negatively charged ions, which are loosely attracted by the particle surface due to the electrostatic force of the charged particle. The highest electrical potential within EDL is observed on the particle surface. The potential gradually drops as one moves further away from the particle surface and reaches zero at the outer boundary of EDL. The electrical potential value at the slipping plane is known as zeta potential (ζ) which is used for determining the stability of a given nanofluid. The purpose of electrostatic stabilization is to increase the potential barrier between two particles so that particles cannot come too close to each other and form strongly bonded clusters. Higher potential barrier leads to superior nanofluid stability (See Fig. 3(a and b)). For improved electrostatic stability, differently charged surfactants (ionic) are added to the nanofluid suspension [87,88]. Surfactant can be classified mainly into four types: (a) *cationic* i.e. Cetyl trimethyl ammonium bromide (CTAB), Benzalkonium chloride (BAC), Cetrimonium chloride (CTAC); (b) *anionic* i.e. Sodium dodecyl sulphate (SDS), Sodium dodecylbenzene sulphonate (SDBS), Ammonium lauryl sulphate (ALS), Potassium lauryl sulphate (PLS); (c) *non-ionic* i.e. Tween 20, Tween 80, Span 80, Poly vinyl pyrrolidone, Pluronic P-123, Brij 700, Triton X-100, Gum arabic, Oleic acid, Oleyl amine, Sodium cholate, Sodium deoxycholate, Rokanol K7, Rokacet O7 [67,89–91]; and (d) *amphoteric* i.e. Lecithin, Hydroxysultaine, Sodium lauroamphoacetate, Coamidopropyl betaine [82]. Amphoteric or zwitterionic surfactants are surfactants which contains both cationic and anionic hydrophilic group in its structure. These surfactants are able to form cation and anion based on the pH of the medium. These surfactants have low toxicity, anti bacterial properties, resistance to hardness of water and are compatible with other types of surfactants.

In addition to the above, the pyrene derivative stabilizers (anionic surfactant) i.e. 1-Pyrenesulfonic sodium salts (Py-1SO_3), 6,8-dihydroxy-1,3-pyrenedisulfonic acid disodium salt (Py-2SO_3), 8-hydroxypyrene-1,3,6-trisulfonic acid trisodium salt (Py-3SO_3), and Tetrasodium 1,3,6,8-pyrene tetrasulfonic acid (Py-4SO_3), 1-Pyrenebutylic acid (PBA), 1-pyrenebutanol (PB), 1- Pyrenecaboxylic acid (PCA) [89,92–96], and aromatic stabilizers (non-ionic surfactant) i.e. polycyclic aromatic hydrocarbons such as tetra potassium salt of coronene tetra carboxylic acid [97] and perylenebisimide based bolaamphiphile detergent [98] are widely used for stabilization of carbon based nanoparticle in different basefluid. Pyrene derivative are also considered as anionic surfactant and fall under non-covalent functionalization approach of nanofluid stabilization. Ionic surfactants (cationic and

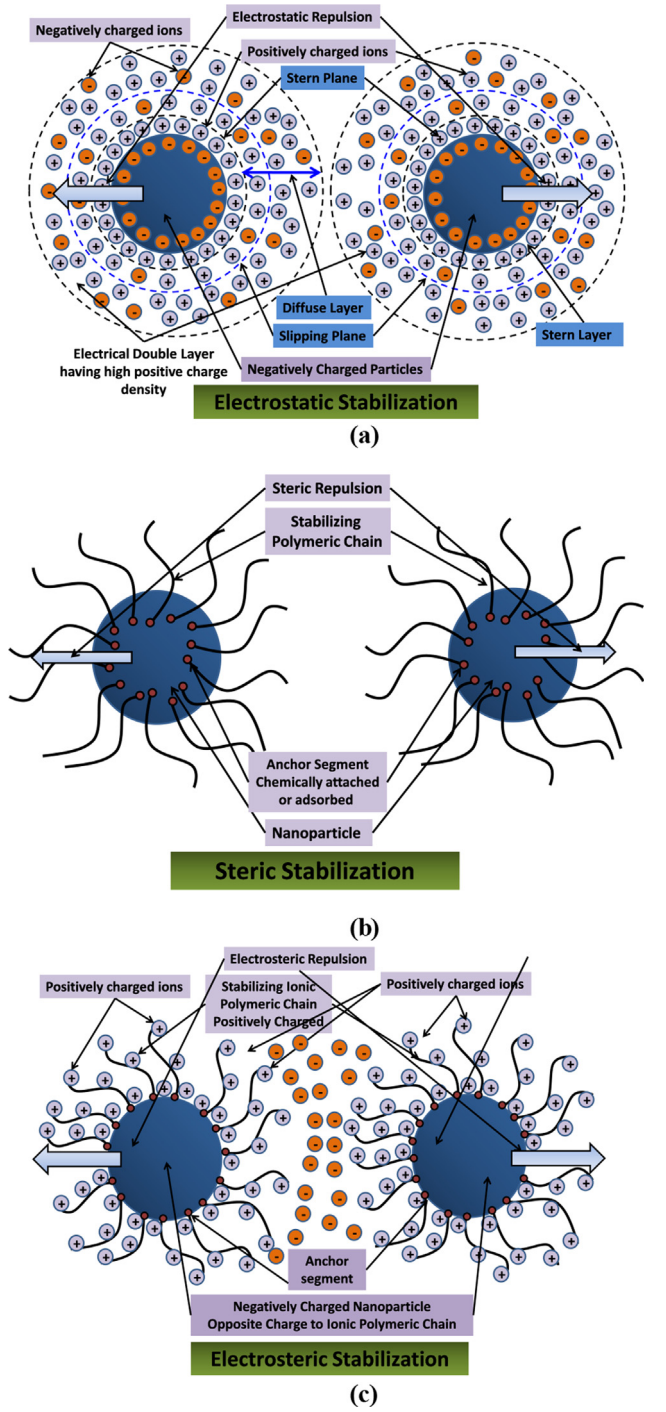

Fig. 9. Schematic representation of (a) electrostatic, (b) steric, and (c) electrosteric [122] stabilization scheme.

anionic) are used in order to achieve electrostatic stabilization and non-ionic surfactants are used for steric stabilization. Non-covalent functionalization can be achieved by various means such as ionic surfactant, non-ionic surfactant, polymer and aromatic surfactant. In case of carbon based nanofluid, the main disadvantage of non-covalent functionalization is that it forms foam inside thermal equipments leading to reduction in effective heat transfer area and thermal performance [99,100]. In some cases, non-covalent functionalization of carbon based nanofluid not only reduces thermal properties but also increases viscosity of nanofluid (GNP-SDBS/water nanofluid) which is detrimental from thermal performance view-point [101]. On the other hand, covalent functionalization overcomes such problems and display good dispersion of carbon based nanoparticle [101–103]. For improving the dispersion stability of carbon based nanoparticles in aqueous/organic solvent, both covalent and non-covalent functionalization is used. The most common stabilizers used for non-covalent functionalization of carbon based nanoparticle are Gum Arabic (GA), Sodium Dodecyl Sulfate (SDS), Sodium Dodecyl Benzene Sulphonate (SDBS) and Triton X-100. Among these four stabilizers, SDBS provides best dispersion of carbon based nanoparticle in water due to strong π-π interaction between carbon nanoparticle [101,104–106].

In addition to ionic surfactant, electrostatic stabilization can be attained by altering the functional groups present on the surface of nanoparticle by acid, alkaline and plasma treatment. Polar functional groups (hydroxyl, carboxylic, carbonyl, sulphate, amine and phosphate etc.) on the nanoparticle surface lead to superior suspension stability in polar solvents. Such type of functionalization is known as the covalent functionalization [89,107]. Covalent functionalization can be subdivided into many classification such as hydroxyl, carboxyl and amine based functionalization. The effect of covalent (using cysteine) and non-covalent functionalization (using Gum Arabic) on the stability of CNT based nanofluid has been studied by Shanbedi et al. [102]. Amine based functionalization of crumpled nitrogen doped graphene nanosheet in water/ethylene glycol based nanofluid was carried out using cyanamide to improve nanofluid stability [108]. Water based graphene quantum dot nanofluid was stabilized for 30 days using amine functionalization without use of any surfactant/polymer [109]. Amine treatment of aqueous graphene quantum dot nanofluid was also reported by Soleymaniha et al. [110] where long-term nanofluid stability was achieved with high thermal performance and negligible fouling effect. Ettefaghi et al. [111] prepared low-cost stable (6 months) water-graphene quantum dots nanofluid using citric acid and urea as precursor. They used hydrothermal technique to prepare cost-effective, eco-friendly stable nanofluid. He et al. [112] reported utilization of graphene quantum dots as stabilizer for stabilizing water based graphene nanofluid.

The stability of nanofluids can also be attained by pH adjustment. In order to maintain high nanofluid stability, the pH value of the system should be maintained at either higher or lower value compared to IEP. At IEP, zeta potential is equal to zero which is undesired from stability view-point (no repulsive force). The enhanced repulsive force is necessary to maintain higher nanofluid stability. At optimum pH level, nanoparticles possess high charge density which is desirable for maintaining well dispersed nanofluid [113,114]. In order to disperse CNT in water, acid treatment is carried out for introducing hydroxyl group on the nanoparticle surface, which helps in converting hydrophobic (CNT) nanoparticle into hydrophilic [16]. Several studies [47,65,66,115] on the effect of pH on nanofluid stability reported that at pH value close to 7, particle tends to agglomerate whereas at higher and lower pH value there is less agglomeration (See Section 6.2). However, from the heat transfer application point of view, too high or too low pH value may lead to accelerated corrosion of heat transfer surface [116].

The effectiveness of different oxidizing agents such as HNO_3, H_2SO_4, $KMnO_4$ in altering the dispersion stability of MWCNT has been discussed by Wepasnick et al. [117] using surface functionalization by polar functional groups [118]. Ghozatloo et al. [33] reported synthesis of water soluble graphene using alkaline based functionalization where, potassium persulfate ($K_2S_2O_8$) was added into aqueous suspension of graphene as the oxidizing agent and potassium hydroxide (KOH) as pH adjusting agent. The graphene nanosheets produced by this method is highly water soluble due to the formation of −OH, −COOH, −COOK functional group at the edges of the graphene sheet. Formation of oxygen containing functional group (polar group) has been confirmed by FTIR analysis. Liu et al. [119] prepared chemically modified single wall carbon nanotube using peroxytrifluoroacetic acid to produce SWNT nanofluid which is soluble in polar solvent (water, ethanol, dimethylformamide) by introducing trifluoroacetic groups (CF_3COO-) and other oxygen based functional groups (−COOH, C═O, C−O) on the

nanoparticle surface. Plasma treatment of diamond nanoparticle was carried out using gas mixture of methane (CH_4) and oxygen (O_2) for introducing polar functional groups such as carbonyl, carboxylic and aldehydes on the nanoparticle surface for improving the dispersion stability in polar medium (water) [120]. Table 5 summarizes the examples of electrostatic stabilization carried out for improving the nanofluid stability. The limitations of electrostatic stabilization are:

(a) This technique can only be useful for dilute nanoparticle suspension.
(b) This method is unsuitable for electrolyte sensitive systems i.e. system having calcium, sodium, and magnesium ion. Electrostatic stabilization technique is also ineffective in saline environment.
(c) Redispersion of the already agglomerated particle is not possible.
(d) This technique is not suitable for non-aqueous suspension.

7.2.2. Steric stabilization

The steric stabilization of nanofluid can also be termed as polymeric stabilization technique which involves addition of polymer molecules in nanoparticle suspension for the purpose of preventing particle aggregation and eventual sedimentation. The polymeric molecules attached to the nanoparticle surface prevent the two nanoparticles from coming close to each other. It creates a steric hindrance which prevents nanoparticles from adhering to each other (See Fig. 9(b)). The steric stabilization of nanofluid can be achieved using non-ionic surfactant and polymer. This stabilization technique falls under non-covalent functionalization [89,102,106,121]. The advantage of using steric stabilization is that it can stabilize nanofluids with high particle concentration which is not possible by electrostatic stabilization.

When polymeric chains get adsorbed on the nanoparticle surface, there is restriction in free movement of the nanoparticle in basefluid, which acts as steric diffusion barrier to prevent nanoparticle agglomeration [122,123]. Polymeric chain length and adsorption ability of polymer plays a crucial role in steric stabilization. Short chain polymer and polymer with poor adsorption properties are ineffective as steric stabilizers. Strong binding (by chemisorptions) between nanoparticle and polymeric chain is essential for achieving steric stabilization. The non-ionic amphiphilic polymer can be used for steric stabilization which is made of two parts, i.e. anchor part which gets attached to the nanoparticle surface and the polymeric tail which interacts with the solvent molecules to prevent two nanoparticles from interacting with each other [122]. Fig. 9(b) shows the anchor part and stabilizing polymeric chain. The stabilizing polymeric chain prevents nanoparticles from adhering to each other by providing a protective layer against the agglomeration. Two factors play major role to achieve steric stabilization in nanosuspensions i.e. strong enthalpic interaction between molecule of the dispersing media and solvated polymeric tail, and length and density of the polymeric tail attached to the nanoparticle surface for minimizing VDW attraction between two approaching nanoparticles [124,125].

Steric stabilization is also known as the thermodynamic stabilization scheme, where total interaction potential can be represented by total Gibbs free energy of system G_T given as [122],

$$G_T = G_A + G_{ST} = G_A + G_{OS} + G_{VR} \quad (23)$$

G_A, G_{ST}, G_{OS} and G_{VR} represent Gibbs free energy of attraction, steric repulsion, osmotic repulsion and volume restraint interaction respectively. Osmotic repulsion/mixing interaction (G_{OS}) is the increase in osmotic pressure by overlapping of polymeric layer surrounding the nanoparticle due to increase in the concentration of solvated polymeric tail near the zone of interaction. Solvent molecules migrate to the zone of overlapping polymer layer due to this effect and generate strong repulsion to prevent nanoparticles from agglomerating. The sign of G_{OS} depends on solvency of the stabilizing polymer in the dispersion medium. A solvent can only be termed as a good solvent from stabilization perspective, when the sign of G_{OS} is positive such that the adverse mixing interaction assists in nanoparticle repulsion and nanofluid stabilization. On the other hand, in case of poor solvent, the sign of G_{OS} is negative and mixing interaction is attractive in nature which will lead to nanofluid destabilization. The value of volume restraint interaction or entropic interaction (G_{VR}) is always positive which means it is favourable from repulsion point of view. Volume restraint interaction can lead to decrease in interacting polymer volume due to overlapping and compression of polymeric chain which results in subsequent decline of entropy. It is to be pointed out that summation of G_{OS} and G_{VR} contributes to repulsive free energy. From the concept of Gibbs free energy, it can be concluded that steric stabilization can be achieved when $\Delta G > 0$. For a good solvent, $G_T > 0$, $G_{ST} = G_{OS} + G_{VR} > G_A$ and for a poor solvent, $G_T < 0$, $G_{OS} + G_{VR} < G_A$ with $\Delta G > 0$ and $\Delta G < 0$ respectively [122,126].

Polymer used in steric stabilization can be either normal/homopolymer consisting of identical monomers or co-polymer consisting of two different monomers incorporated in single polymeric chain. Copolymer can also be classified into three sub-types namely random, block and graft type. Random co-polymer is a type of polymer made of multiple types of monomer units arranged together in a random manner whereas a block copolymer is a polymer formed when two monomers forms blocks of repeating units. Graft copolymer is different from random and block copolymer where linear backbone is made of one monomer and side chain is made of another monomer. Amphiphilic block or graft copolymers are ideal for steric stabilization. The criteria behind choosing copolymer for steric stabilization are: one part of the polymer should have affinity towards the suspended nanoparticle (gets attached to nanoparticle surface by chemisorptions or physisorption) and the other part is compatible with the dispersion media [127]. Greater steric stabilization properties is achieved by providing anchor polymer (particle loving monomer) and stabilizing moieties (solvent loving monomer). For aqueous dispersion, polystyrene-polyoxyethylene (anchor polymer-stabilizing moieties), polyvinyl chloride-polyvinyl pyrrolidone (PVP), polyvinyl acetate-polyvinyl alcohol, polyacrylonitrile-polymethacrylic acid, polypropylene-polyvinyl methyl ether can be used as copolymer whereas for non-aqueous dispersion polyacrylonitrile- polystyrene, polyvinyl chloride-polyisobutylene, polyoxyethylene-polylauryl methacrylate, and polypropylene-polydimethylsiloxane etc. are used as copolymer. In addition to the above, Gum Arabic, PVP, Triton X 100, Tween 20, Span 80, Oleylamine, Oleic acid are also used widely for steric stabilization [128–132]. The adsorption of long chain non-ionic surfactant (amphiphilic) on the nanoparticle can also provide steric stabilization in both polar and non-polar dispersing medium. The amphiphilic nature (one part hydrophilic and other part hydrophobic) of surfactant makes it ideal (like co-polymer) for steric stabilization. Using non-ionic surfactant like Triton X-100, steric stabilization of both hydrophilic and hydrophobic nanoparticle can be achieved in different basefluid (polar or non-polar solvent) [131,133]. Schematic diagram of steric stabilization using long polymer chain is depicted in Fig. 9(b).

Steric stabilization cannot be quantified using zeta potential measurement since polymer attachment to the nanoparticle surface does not change the surface potential. Therefore, long term sedimentation, centrifugation, UV spectrophotometer, transmittance, or DLS techniques can be implemented to quantify the stability. The primary advantages of steric stabilization are that agglomerated particles can be dispersed, and this technique is suitable for stabilization of high concentration nanofluid suspension, electrolyte sensitive system, and multiphase system. Table 5 reports effectiveness of steric stabilization for different types of nanofluid.

7.2.3. Electrosteric stabilization

Electrosteric stabilization is an amalgamation of both electrostatic and steric stabilization. In this approach, ionic polymer gets adsorbed on the surface of any charged nanoparticle which leads to the creation of both protective polymeric barrier (steric hindrance) and electric

potential barrier (electrostatic repulsion) between two approaching nanoparticles. In addition to steric hindrance, significant double layer repulsion is generated by the ionic polymer which further improves the stability of the nanofluid. Electrosteric stabilizers are generally ionic polymers which are made of two parts; a) anchor segment and b) stabilizing ionic polymeric chain (See Fig. 9(c)). The anchor segment and stabilizing ionic polymer chain provides both steric and electrostatic stabilization. The polymer used for this purpose is known as polyelectrolyte which is made of repeating polymer units having an ionisable group (carboxylic, sulfonic acid group etc.). Polystyrene sulfonic acid, poly(1-vinylpyrrolidone-co-acrylic acid), polyacrylic acid-block-poly butyl acetate, polyvinyl sulfonic acid, and poly(methacrylic acid) etc are examples of electrosteric stabilizers [122,134]. The ionizable group gets dissociated in the dispersing media to form an electrically charged polymer. In order to achieve good polymer adsorption on the nanoparticle surface, both nanoparticle and polyelectrolyte should be of opposite charge as shown in Fig. 9(c). Polyelectrolytes having both cationic and anionic groups are known as polyampholyte which can provide electrosteric stabilization. Ionic liquids can also be implemented to achieve electrosteric stabilization due to its high charge density (to provide electrostatic stabilization), and strong chemisorptions on the nanoparticles surface (to provide steric repulsion). Imidazolium, pyridinium, tetrafluoroborate and hexafluorophosphate are few examples of ionic liquid used for nanoparticle stabilization [122,135].

Kong et al. [136] used strong anionic polyelectrolyte (melamine formaldehyde sulfonate, MFS) and non-ionic polymer (hydroxypropylmethylcellulose, HPMC) to electrosterically stabilize cement particles in DI water medium. Authors reported poor performance of MFS as stabilizer as cement particles can only be dispersed in water for a short time period after which particles refloculate. However, superior stabilization was observed using both MFS and HPMC. Fig. 9(c) shows the mechanism behind electrosteric stabilization using polyelectrolyte.

8. Effect of operating conditions on stability

Application of nanofluid stretches from manufacturing [36,148], electronics cooling [149,150], solar power [151,152], nuclear power plant [153], heat exchangers [154,155], microfluidics [156,157], automobile [158] to enhanced oil recovery [10,159,160] etc. The stability of nanofluid gets altered during operation due to change in operational conditions i.e. temperature, salinity, confinement and shear etc. The effect of operational conditions on stability of nanofluid and possible remedial actions are reviewed in the following sections for several applications.

8.1. Stability effect in heat transfer applications

Nanofluid undergoing heating and cooling cycle during operation can lead to particle agglomeration. Particles suspended in a basefluid have higher Brownian motion during the heating cycle as the particle diffusion coefficient is directly proportional to fluid temperature. High diffusion coefficient implies more particle-particle collision and higher probability of particle aggregation. Therefore, high temperature applications require additional care to suppress instability of nanofluid.

Majority of nanofluids are stabilized via surfactant and polymer addition [22,129,130,161]. However, it may be noted that surfactant and polymers tend to degrade at elevated temperature which detrimentally impacts the nanofluid stability [162]. High temperature stability of both polymeric stabilizer and surfactant needs to be considered for successful use of nanofluid in heat transfer application. Nanofluid should remain stable over a wide range of temperature. The bulk of the study on nanofluid stability at higher temperature has reported significant agglomeration tendency and irreversible deterioration of nanofluid [163,164]. Chang et al. [165] observed that with increase in temperature, nanoparticles tend to form cluster and there is an increase in average particle size. They also observed that zeta potential value of

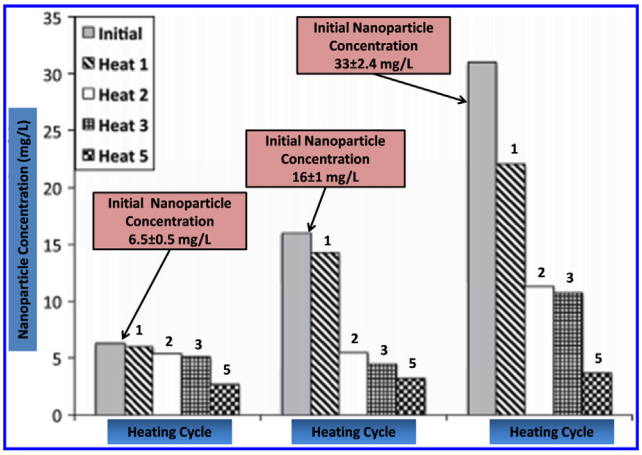

(a)

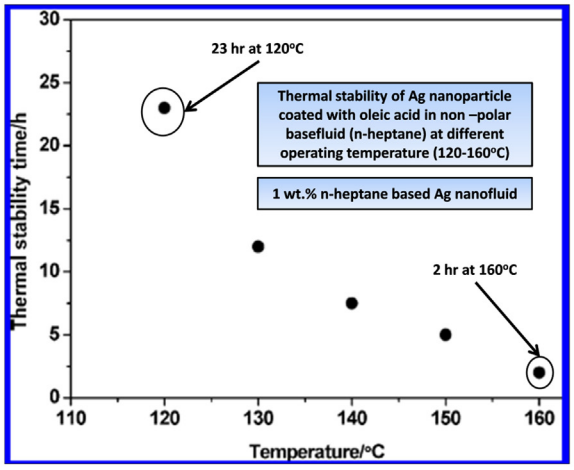

(b)

Fig. 10. Effect of heating cycle and temperature on the stability of nanofluids: (a) effective concentration of MWCNT nanoparticle in Therminol VP-1 basefluid after 5 heating cycle (heated at 220 °C for 1 h) [167], and (b) effect of operating temperature on stability time of n-heptane based Ag nanofluid [5].

CuO nanofluid decreases from 21.7 mV to 13.4 mV at 60 °C and 60 min operations which is an indication of reduced stability. To ensure high temperature nanofluid stability, both mechanical (high pressure homogenizer) and plasma (surface functionalization) treatment can be implemented. Tavares et al. [163] reported synthesis of thermally stable (up to 150 ^{O}C) Cu-EG nanofluid using single step plasma treatment without any surfactant. The agglomeration takes place at 197 °C (close to boiling point of EG) due to enhanced Brownian motion and particle-particle collision. These soft agglomerates can be easily broken down by ultrasonication contrary to the surfactant based stabilization, where aggregation is irreversible. Sani et al. [166] reported the synthesis of stable ethylene glycol based single wall carbon nanohorn nanofluid using high pressure homogenizer (up to 1000 bar), and reported stability of nanofluid till temperature of 150 °C over a period of six months.

Hordy et al. [167] studied both long-term and high temperature (up to 220 °C) stability of MWCNT nanofluid for different basefluid such as water, ethylene glycol, propylene glycol, and Therminol VP-1. It was observed that except Therminol VP-1 based MWCNT nanofluid, all other basefluids show long-term nanofluid stability over a period of 8 months. Fig. 10(a) shows the impact of heating cycle on the stability of Therminol VP-1 based MWCNT nanofluid at three different initial concentrations (6.5 ± 0.5, 16 ± 1 and 33 ± 2.4 mg/L). It is observed that after completion of each heating cycle, nanoparticle concentration keeps on reducing for all three initial concentrations which

can be interpreted as poor nanofluid stability at high temperature (220 °C) in therminol VP-1 medium. It may be noted that all other basefluids except Therminol VP-1 are polar in nature which plays crucial role in long term stability aspect of MWCNT nanofluid. MWCNT used in this study were treated with plasma which grafted oxygenated functional groups (carboxylic and hydroxyl) on the particle surface. MWCNT nanoparticle is more compatible with polar solvents (water, ethylene glycol, polyethylene glycol) due to plasma induced functionalization.

Li et al. [5] investigated the influence of temperature on the stability of n-heptane based oleic acid coated silver nanofluid. It was observed that Ag nanofluid is stable for months when used at room temperature and the thermal stability duration reduces from 23 h at 120 °C to 2 h at 160 °C. Fig. 10(b) shows sample results on effect of temperature on stability of n-heptane based Ag nanofluid.

Nanoparticle deposition on the heat transfer surface due to loss of stability can contribute to additional heat transfer resistance in the form of fouling factor [27,28,30,31]. Sarafraz et al. [30] observed higher heat transfer coefficient and improved thermal performance of thermosyphon using water-TiO_2 nanofluid during the initial period. However, when the study was extended over long time duration (14,000 min) particulate fouling resulted in reduction of heat transfer. The effect of particulate fouling gets further intensified at higher heat load, weight fraction and angle of inclination of thermosyphon. Negative impact of nanoparticle fouling on flow boiling heat transfer coefficient was reported for MgO-therminol 66 nanofluid at high nanoparticle concentration [168]. In another study, Sarafraz et al. [35] reported the thermal performance of COOH functionalized CNT-water nanofluid in a counter current heat exchanger and observed increase in pressure drop of 11% and augmentation in thermal conductivity up to 56% with overall improvement in thermal performance index (η) by 44%. Nanofluid used for this study showed good stability over a period of 21 days using Nonylphenol ethoxylate (NPE) as stabilizer. This investigation was conducted for a wide range of Reynolds number (Re = 900–10,500) at temperature range of (50–70 °C) confirming the effectiveness of nanofluid at high temperature and different flow regimes. Sarafraz et al. [169] also reported thermal performance and viscosity of Ag-coconut oil nanofluid under convective boiling scenario inside an annular heat exchanger. In comparison to water based or ethylene glycol based nanofluid, this nanofluid showed negligible fouling even after 1000 min with lower particle clustering tendency due to lower evaporation rate of coconut oil compared to other basefluid.

Nanoparticle deposition on heat transfer surface can lead to increase in surface roughness which aids in nucleate boiling heat transfer [1,36,170]. The effect of flow condition inside channel, pipe, heat exchanger on nanofluid stability and subsequent effect on heat transfer has been extensively investigated by many researchers for several nanoparticle and basefluid combinations [28,31,34,35,171]. Lin and Yang [172] have discussed about the flow instability of nanofluid under elevated temperature and reported that nanofluid becomes unstable as it changes its flow regime from laminar to turbulent flow.

The wall effect on the thermal performance of nanofluid under strong temperature gradient has also been studied by some researchers [173,174]. There is significant impact on the thermal performance and thermo-physical properties of nanofluid due to near wall velocity gradient. However, more experimental and theoretical studies are warranted to understand the impact of surface properties and flow rate on the performance of nanofluid under strong temperature gradient.

8.1.1. Impact of nanofluid stability on thermo-physical properties

Among several beneficial attributes of nanofluid, thermal conductivity and viscosity are considered to be of paramount importance from the context of its industrial large scale applicability. However, the main bottleneck behind large scale implementation of nanofluid lies in the effect of stability on nanofluid properties i.e. thermal conductivity, viscosity, specific heat and surface tension.

The thermal conductivity of stable nanofluid suspension is higher than the thermal conductivity of destabilized nanofluid [6,175]. In addition to the uniform dispersion case of nanofluid, the optimum level of clustering for high thermal conductivity has been discussed by several researchers [21,55,176]. Wen et al. [177] and Prasher et al. [55] reported the optimum aggregation level required to attain maximum thermal conductivity enhancement which contradicts the concept of homogeneous dispersion. Prasher et al. [55] observed that the nanoparticle clusters are made of both linear and side chains. The enhancement in thermal conductivity is attributed to linear chain like structure which helps in heat conduction. Timofeeva et al. [178] also observed that nanoparticle aggregation is one of the contributing factors for increase in thermal conductivity. However, larger aggregate or cluster formation can lead to sedimentation and drop in thermal conductivity of nanofluid. Therefore, it is essential to control the rate of aggregation so that stability remains unchanged over a long duration by stabilizer addition, functionalization, pH control or ultrasonication. The effect of stabilizer addition or other stabilization technique on stability and thermal conductivity of nanofluid has been reported by several researchers [37,79,115,179–181]. The effect of Gum Arabic (GA) on the stability and thermal conductivity enhancement of MWCNT nanofluid was reported by Sadri et al. [79]. Chakraborty et al. [37] observed that addition of SDS improves the zeta potential value (indication of superior stability) and thermal conductivity of Cu-Zn-Al LDH nanofluid. Su et al. [181] reported the effect of sonication time on the thermal conductivity and stability enhancement of graphite-oil nanofluid. Wei et al. [179] reported stability of diathermic oil based TiO_2 nanofluid over 10 days without using any stabilizer at higher temperature (20–50 °C). Li et al. [115] reported the effect of both pH altercation and surfactant addition on the stability and thermal conductivity of Cu-H_2O nanofluid. Their study revealed that as the pH value increases from 3 to 9.5; there is increase in zeta potential value leading to better stability. When the pH of the suspension is higher compared to the Isoelectric point (IEP), the hydration force between nanoparticles increases leading to greater mobility. Enhanced particle mobility results in microconvection which helps in heat transfer augmentation. Addition of SDBS surfactant to nanofluid suspension with pH value in the range of 8.5–9.5 leads to thermal conductivity enhancement. However, there is a drop in thermal conductivity value with subsequent increase in pH value. The optimal balance between pH and surfactant addition is desired to achieve good particle dispersion and heat transfer properties.

Limited studies of nanofluid stability effect on specific heat capacity are available in literature contrary to that of thermal conductivity. Specific heat capacity of nanofluid decreases with increasing particle concentration [82,182,183]. More systematic study is required to understand the effect of nanofluid stability on specific heat capacity.

The particle aggregation can also detrimentally impact the rheological characteristics of nanofluid. The impact of particle clustering on viscosity of nanofluid has been discussed in details by Duan et al. [184]. It was observed that nanofluid behaves like Non-Newtonian fluid due to excess clustering which then behaves like Newtonian fluid after sonication. Both ultrasonication and stabilizer (CTAB) were used to ensure long term stability. Microstructure of dried nanoparticles from SEM measurement showed distinct difference in particle aggregation before and after ultrasonication. The change in rheological behaviour of nanofluid after ultrasonication indicates the relation between stability and rheological behaviour of nanofluid. Nanofluid can behave both as Newtonian[185] or Non-Newtonian [32,186–188] fluid depending on particle type, concentration, size, basefluid, stabilizer, shear rate and temperature. Irrespective of nanoparticle and basefluid type, nanofluid viscosity increases with increase in nanofluid concentration and decreases with increasing operating temperature [1,58,183,184,189–192]. Particle size also plays a crucial role on the extent of viscosity enhancement of nanofluid [187,193].

Few studies have reported the effect of nanofluid concentration and operating temperature on surface tension value

[21,32,36,183,194,195]. The surface tension value increases with increase in nanoparticle concentration and deceases with increase in operating temperature. However, in some cases both increase and decrease in surface tension value can be observed with increasing nanofluid concentrations [21,36,196]. More number of nanoparticle leads to lower interparticle gap and higher Van der Waal attraction in liquid air interface leading to increase in surface tension. The surface tension value can reduce at low particle concentration due to electrostatic repulsive force or nanoparticle alignment at liquid-air interface. This phenomenon can also be governed by the nature of nanoparticle (hydrophilic or hydrophobic) and basefluid. However, excessive clustering can also lead to sedimentation and reduction in surface tension value as the particle concentration reduces in bulk media.

8.1.2. Price-performance analysis of nanofluid

The favorable properties of nanofluid lead to superior performance of several applications. However, a cost is also associated with synthesis of nanofluid. Therefore, price performance analysis of nanofluid should be undertaken for selection of nanofluid. The reduction in thermal properties due to instability can influence price performance factor of nanofluid. The industrial applicability of nanofluid is only possible when cost of nanofluid is lower than the saving due to performance improvement i.e. the thermal conductivity ratio is moderately high over a long period of time. Maintaining high thermal conductivity ratio after multiple heating/cooling cycles is of utmost importance for its application in heat transfer. The price performance factor (PPF) of nanofluid is related to the thermal conductivity ratio of nanofluid compared to base fluid and price of the nanofluid. Therefore, reduction in thermal conductivity ratio due to particle aggregation, sedimentation or deposition leads to decease in price-performance factor. Nanofluids having lower particle size usually have higher production cost and superior thermal conductivity ratio. The cost of nanofluid also depends on the price of nanoparticle material i.e. metal and carbon based nanoparticles have high cost whereas metal oxide based nanofluid has lower synthesis cost. Alirezaie et al. [197] carried out PPF assessment of MgO-EG and Fe-EG nanofluid and reported that MgO-EG nanofluid has higher price performance factor compared to Fe-EG nanofluid. The price performance factor is defined as (Alirezaie et al. [197])

$$\text{Price Performance Factor (PPF)} = \frac{\text{Thermal Conducivity Ratio}}{\text{Price of Nanofluid } \left(\frac{\$}{\text{litre}}\right)} \times 1000 \quad (24)$$

where thermal conductivity ratio is the ratio of the thermal conductivity of nanofluid to basefluid. Hemmat Esfe et al. [198] reported that the cost of carbon nanofluid is significantly higher than metal oxide and hybrid nanofluid. The enhancement in thermal conductivity is higher at higher particle concentration i.e. carbon based (SWCNT) nanofluid should be implemented at higher concentration. On the other hand, at low particle concentration hybrid nanoparticle (ZnO-SWCNT) shows more promise compared to individual ZnO and SWCNT nanofluid [198]. Ensuring good nanofluid stability over a long-period of time is key to maintaining high thermal conductivity ratio and price performance factor during the life period of a thermal system.

8.2. Confinement effect in microfluidics applications

Flow of nanofluids inside microcapillary or mini channel has several applications i.e. drug delivery system [199], heat transfer [200], manufacturing [201,202] etc. Unwanted particle sedimentation or particle aggregation can influence the flow of nanofluid through the microchannel. Increase in resistance to fluid flow leads to increase in pressure drop and high pumping cost. A numerical study on the thermal performance and pressure drop calculation of CuO-water nanofluid in a trapezoidal microchannel revealed that with increase in nanoparticle size (100–200 nm), pressure drop increases from 3% to 15% whereas average Nusselt number decreases by 5.3% [203]. Higher particle size implies higher pressure drop and lower thermal performance in microchannel. Sarafraz and co-workers studied applicability of graphene-water [204] and graphene-water/ethylene glycol (60:40) [34] nanofluid in microchannel and reported improved thermal performance index with an increase in pressure drop, friction factor and pumping cost. These studies revealed the importance of flow rate and particle concentration on overall thermal performance of nanofluid inside a microchannel. The effect of fouling formation on heat transfer performance inside a rectangular microchannel was studied by Sarafraz et al. [205] using carbon nanotube-water nanofluid. It was observed that thermal resistance caused by fouling is strongly dependent on duration of operation and nanoparticle concentration. Higher period of operation and particle concentration leads to greater thermal resistance due to fouling.

Higher sedimentation and fouling formation in microfluidics application is attributed to greater surface effects due to stronger interaction between particle and channel wall. Therefore, the Van der Waal attraction and electrostatic repulsion force between particle and channel wall plays dominant role compared to particle-particle interaction. In case of microchannel flow, particle-particle interaction gets overshadowed by the particle-wall interaction.

In addition to channel geometry, near wall flow dynamics influences the stability of nanofluid in a microchannel. The effect of microchannel geometry on the heat transfer, friction factor of nanofluid has been investigated by several researchers [206,207]. Byrne et al. [208] showed that addition of surfactant (CTAB) in nanofluid (CuO nanoparticle) can enhance the heat transfer performance in a microchannel. Surfactant addition not only stabilizes the nanofluid suspension but also prevents average particle cluster size from increasing with time through electrostatic stabilization. However, the detailed study about the effect of wall and particle interaction on nanofluid stability is limited. Interaction between nanoparticle and channel wall based on the particle shape should also be considered as it could affect the total interaction potential responsible for nanofluid stability (See Sections 5 and 6.4). More investigation is required to understand the impact of confinement, wall-particle interaction and nature of wall surface on the nanofluid stability in microchannel flow.

8.3. Salinity effect in enhanced oil recovery

Several authors have reported that nanofluid is effective in enhanced oil recovery (EOR) applications [9,10,159,160,209]. Factors such as wettability change, reduced interfacial tension of oil-water system, change in disjoining pressure, lower oil viscosity, increase in water viscosity, higher film and slug dislocation, and log jamming are responsible for EOR using nanofluid [10,160,209,210]. Log jamming is the manifestation of pore blockage by nanoparticle aggregation and forced production of oil from adjacent pores where oil was trapped previously.

It is not possible to achieve all the benefits of enhanced oil recovery using naked nanoparticle suspension in basefluid. ShamsiJayezi et al. [160] reported that polymer and surfactant coated nanoparticle suspension perform better in EOR recovery compared to naked nanoparticle suspension due to several factors such as superior solubility, stability, and easy transport through a porous medium. Polymer coated nanoparticles have greater control over the mobility of injected fluid. In order to ensure good mobility control, viscosity of the injected fluid should be higher than the viscosity of oil. This generates a piston like effect inside the oil reservoir and leads to displacement of more oil from injection to production well. Therefore, in order to ensure greater oil recovery, injected fluid viscosity should be higher than oil viscosity to prevent viscous fingering and low oil recovery [160]. Incorporation of surfactant and polymer along with nanoparticle can lead to the formation of foam or emulsion inside the reservoir which can increase the viscosity of the injected fluid. The high viscosity of the injected phase is

considered good for mobility control. Foam and emulsion also display a shear thinning nature which is advantageous for applying injection fluid at a higher injection rate. Implementation of surfactant and polymer coated nanofluid can also lower down the interfacial tension and alter the rock wettability.

In order to ensure effectiveness of EOR using nanofluid, nanofluid must be able to penetrate deep inside the rock pores to aid in oil production. However, there are several difficulties in transport of nanoparticles through porous medium both with (polyacrylic acid, polyvinyl pyrrolidone, cellulose, surfactant) and without stabilizers [211–213]. Formation of large particle aggregates can hinder the applicability of nanofluid in low permeable rock formation. When the cluster size is higher than the pore size of rock, particles can block the pores. This phenomenon is called physical filtration which can happen with both well dispersed and aggregated particle suspension depending on the permeability of rock. For non-aggregated particle suspension, such filtration can take place depending on size, shape, aspect ratio and polydispersity of the suspension. Bayat et al. [214] showed that metal oxide based nanofluid used for enhanced oil recovery gets deposited on the limestone rock surface. The adsorption of TiO_2 and SiO_2 nanoparticle can alter the wettability of the rock surface which is beneficial for enhanced oil recovery. However, excessive nanoparticle adsorption on the rock surface and pore areas can increase the cost of enhanced oil recovery as lesser amount of nanoparticle can be recovered after it passes through the porous media. In addition to that more particle deposition can also block the pore areas which are essential for oil flow towards the production well and deep penetration of injected fluid for oil recovery. The excessive nanoparticle deposition and pore area blockage is related to the nanofluid stability in porous medium.

The condition inside the oil reservoir has high salinity, which is detrimental on the stability of suspended nanoparticles. Increase in salinity influences the zeta potential value of nanofluid by compressing the electrical double layer and lowering the electrostatic repulsive force. Al-Anssari et al. [215] reported that with increase in NaCl concentration, zeta potential value of SiO_2 nanofluid decreases from −45 mV to 0 mV which is an indication of deterioration in nanofluid stability. Fig. 11 shows the effect of salinity on the zeta potential value of SiO_2 nanofluid i.e. the zeta potential value reduces with increase in salinity.

Effect of saline condition can be countered by coating the nanoparticles with polymer or surfactant which provide adequate electrostatic or steric stabilization of nanofluid. Using highly acidic polyelectrolyte such as polystyrene sulphonate, zwitterionic sulfobetaine, poly (2-Acrylamido-2-methyl-1-propanesulfonic acid) (poly AMPS), polyacrylic acid, and bilayer coating of ionic surfactant, sufficient electrostatic stabilization can be provided [160,213,216]. It is to be pointed out that non-ionic and less-acidic polymeric stabilizers such as polyethylene glycol, polyacrylamide, and polyvinylpyrrolidone do not perform well under high temperature and high salinity condition. The stability of nanofluid is also highly pH sensitive. Both high salinity and presence of bivalent ions can hinder the stability of nanofluid inside the oil reservoir [145]. Bagaria et al. [145] reported high zeta potential value (−45 mV) of iron oxide nanoparticle coated with poly (2-acrylamido-3-methylpropanesulfonate-co- acrylic acid) (poly AMPS-co-AA) in silica sandstone under saline environment (8 wt% NaCl and 2 w% $CaCl_2$) indicating high nanofluid stability. The coating not only improves suspension stability by means of electrosteric stabilization but also reduces nanoparticle adsorption on silica sandstone. Foster et al. [216] reported good stability of iron oxide nanoparticle using Poly (AMPS) as stabilizer up to 1 week (at 90 °C) under saline condition (8 wt% NaCl and 2 w% $CaCl_2$) in silica and berea sandstone. Iqbal et al. [146] reported 30 days stability of magnetite nanoparticle using copolymer of AA and AMPS under high salinity (8 wt% NaCl and 2 wt% CaCl2) and high temperature (120 °C) condition. Long chain polymer (cellulose, starch, and polyacrylamide) coating on nanoparticle surface can also provide good steric stabilization of nanoparticle suspension under saline environment [217].

8.4. Magnetic field effect

Self-assembly property of magnetic nanofluid has its application in several systems such as drug delivery [121,218], patterning [219], magnetic levitation [220], and photonics [221]. Several researchers have reported the effect of magnetic particle aggregation under magnetic field [222,223]. The effect of particle aggregation under magnetic field has both beneficial and detrimental effect based on its field of application. Magnetic field induced particle aggregation is favourable in drug delivery, magnetic levitation, photonics and drying applications [199,202,221,224]. Asfer et al. [200] have reported that convective heat transfer coefficient may increase or decrease under the influence of magnetic field depending on factors such as (a) ratio of magnetic force to inertia force, and (b) increase in local thermal conductivity of ferrofluid due to chain like cluster formation.

Chang et al. [225] studied the effect of magnetic field on the stability of CuO nanofluid. The CuO nanofluid loses stability at a faster rate in the presence of magnetic field. The repulsive potential acting between two suspended particles diminishes leading to higher nanoparticle aggregation. Formation of coarse particle (depicted via TEM image and particle size measurement) takes place under the effect of magnetic field. Average particle size increases whereas zeta potential value decreases under the influence of strong magnetic field which is a clear indication of clustering tendency and poor stability.

Parker et al. [226] reported aggregation of the paramagnetic particle under the influence of a strong magnetic field. They used particle suspension of $Mn_2P_2O_7$, Mn_2O_3, MnO, and Cr_2O_3 to measure the impact of magnetic field on particle aggregation. Settling velocity of all the suspended particles increased significantly under the influence of vertical magnetic field. Gareev et al. [227] reported the formation of chain like structure in Fe_3O_4/SiO_2 nanofluid under constant magnetic field using Atomic Force Microscopy (AFM). Wang et al. [228] reported the formation of different colloidal assembly under the influence of magnetic field.

Magnetic nanoparticles should retain its stability after removal of the imposed magnetic field. In order to maintain the magnetic nanofluid stability and to ensure its reusability, electrostatic or steric stabilization technique has to be implemented. Several researchers [200,229–232] have used oleic acid as a dispersant in order to maintain the stability of magnetic nanoparticle for longer duration. Fig. 12(a–d) shows the selected TEM image of the monodisperse and ordered iron

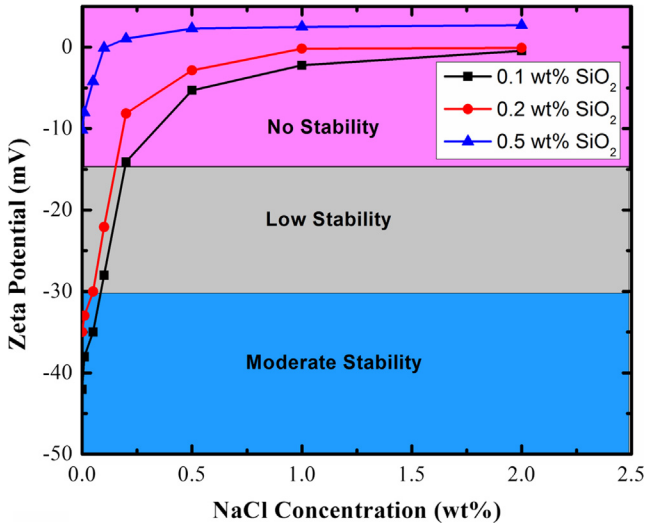

Fig. 11. Effect of salinity on the zeta potential value of water-SiO_2 nanofluid [215].

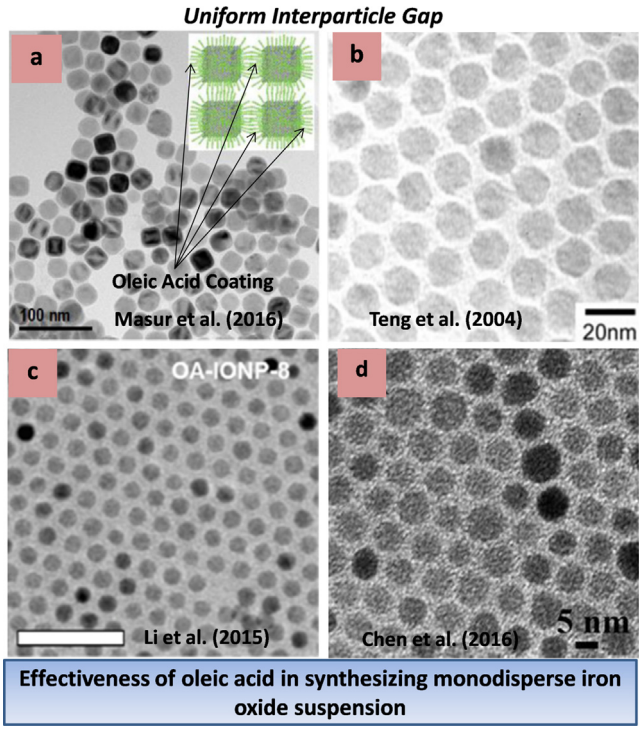

Fig. 12. Selected TEM images of monodisperse iron oxide particle suspension using oleic acid [229–232].

oxide nanoparticle coated with oleic acid indicating improved suspension stability. The oleic acid chain attached with the iron oxide nanoparticle surface prevents individual particles from adhering to each other by steric stabilization [229–232].

8.5. Shearing effect in drag reduction applications

Nanoparticles present in nanofluids can create a film on the lubricating surface leading to energy saving by lowering the friction and wear in different types of industrial systems. Zhou et al. [233] reported that Cu nanoparticle in oil medium perform better as friction and anti-wear reducing agents than zinc dithiophosphate under high load bearing condition at an elevated temperature. According to the authors, the enhanced tribological properties of Cu nanoparticles can be interlinked to the thin particle film having low elastic modulus and hardness. Abdulbari et al. [234] reported drag reduction properties of bismuth oxide (Bi_2O_3), titanium oxide (TiO_2), iron oxide (Fe_3O_4), silica (SiO_2) nanofluid in a microchannel. The percentage drag reduction (DR) is calculated by measuring the pressure drop (using pressure transmitter) in a microchannel before and after nanofluid addition. Authors reported that nanoparticles having high rigidity show good friction reduction features when suspended in liquid medium.

Drag reduction feature of nanofluid is linked with several factors i.e. flow rate (Reynolds number, Re), rheological nature (Newtonian/ shear thinning/shear thickening), nanoparticle concentration, nanoparticle size, shear rate, shear duration and surface roughness. Percentage drag reduction is greater for nanoparticle having a smaller size. Wu et al. [235] studied the effect of drag reduction by dispersing TiO_2 nanoparticle in engine oil using paraffin oil as dispersant and reported that particle size of TiO_2 influences the reduction in friction force. TiO_2 nanofluid having a particle size of 59 nm produces lower friction coefficient than nanofluid having particles of 83 nm. Witharana et al. [236] investigated the effect of different operating conditions such as particle concentration (0.5–8 wt%), shear rate (500–3000 s^{-1}), temperature (20–60 °C) and shear duration (5–40 min) on the stability of TiO_2-EG nanofluid. They observed that under the effect of high shear rate (3000 s^{-1}) and elevated operating temperature (60 °C), TiO_2 nanoparticle size increased from primary size of 25 nm to a maximum average cluster size of 132 nm. However, it was also observed that by varying shear rate from 500 to 3000 s^{-1}, the average cluster size only varies between 126 and 132 nm which is relatively insignificant. The effectiveness of SiO_2 nanofluid in drag reduction is more pronounced on the rough surface as reported by Pouranfard et al. [237]. In case of rough pipe, percentage drag reduction is higher for identical Re and pipe diameter compared to smooth pipe. The drag reduction performance of nanofluid is influenced by flow rate, surface roughness and nanofluid concentration. In turbulent regime, drag reduction using nanofluid is more prominent than in laminar regime [8]. The mechanism of drag reduction using nanofluid is attributed to modification in surface characteristics by nanoparticle deposition. In case of rough pipes, nanoparticle deposits on the pipe wall improve the pipe smoothness and helps in drag reductions. However, nanoparticle deposition may not be effective from surface modification view-point in smooth pipe [8,237]. Sarafraz et al. [169] reported the beneficial attributes of Ag-coconut oil nanofluid in lubrication of high friction surface at high operating temperature and low concentration of nanoparticle. Low fouling formation (thin nanoparticle layer on rough surface improves interlayer movement and lubrication) of nanofluid leading to enhanced lubricating properties. However, at a high particle concentration, nanoparticle clustering and excessive sedimentation/ deposition are undesired for drag reduction. Therefore, optimum nanoparticle concentration and nanofluid stability should be considered.

In addition to stability, rheological properties of the nanofluid also plays significant role in its drag reduction characteristics. Scientific opinion on the rheological behaviour of different nanofluids contradicts each other. Some literature claim that nanofluid display Newtonian behaviour [185] whereas others have observed the non-newtonian behaviour [32,186,187]. It may be pointed out that rheological features can differ based on the shear rate at which nanofluids are tested. At high shear rate, Newtonian behaviour is expected whereas at low shear rate value, nanofluid can show both Newtonian and non-newtonian behaviour depending on properties and interaction between basefluid and nanoparticles. Chen et al. [185] reported the effect of shear rate on the stability and viscosity of TiO_2-EG nanofluid. The rheological analysis carried out for this study shows Newtonian behaviour of TiO_2-EG nanofluid over a large shear rate range of 0.5–200 s^{-1}. The rheological behaviour of nanofluid may also vary based on particle shape and particle concentration [185,238]. Aladag et al. [186] studied viscosity of water based Al_2O_3 and CNT nanofluid at low temperature (2–10 °C) for different shear duration (120–240 s) and variable shear rates (5–4000 s^{-1}). When nanofluid is subjected to high shear rate, nanoparticle clusters tend to break down rapidly which leads to decline in viscosity. When the process is reversed i.e. reduction in shear rate leads to formation of nanoparticle network and increase in viscosity. In addition to shear rate, increasing shear duration also lead to rebuilding of the initial nanoparticle cluster which is undesired from drag reduction point of view. According to the literature, drag reduction is favoured for non-newtonian (shear thinning) fluid [8,86,239]. Yanuar et al. [8] reported the effectiveness of alumina nanofluid in drag reduction under turbulent flow condition. They concluded that higher mixing time and higher particle concentration leads to better drag reduction performance.

Stability of nanofluid plays a critical role in determining effectiveness of nanofluid as drag reducing agent for both short-term and long-term basis. Depending on the operating condition and the nature of the basefluid, steric or electrostatic stabilization can be implemented. Surfactant and polymer used for nanofluid stabilization can also acts as a drag reduction agent by altering the rheological nature and chemical nature of pipe wall by adsorption or deposition. The polymer and surfactant present in the basefluid tend to form network or micelles under flowing condition which contributes to viscoelastic effect responsible for drag reduction. However, it may be noted that under closed loop

condition, effectiveness of polymer is uncertain as it degrades under high stress inside pumps and its effectiveness gets nullified. Both surface active nature and micelle formation feature of surfactant contributes to drag reduction. Contrary to polymer, effectiveness of surfactant under high stress remains unhindered due to the self-regenerative nature of micelles [86]. Drzazga et al. [86] reported drag reduction using non-ionic surfactant stabilized (Rokacet O7 and Rokanol K7) copper oxide nanofluid. The sole effect of nanoparticle addition on drag reduction becomes insignificant when compared to surfactant added nanofluid suspension. Similar to the above study, Liu and Liao [240] reported the effectiveness of CTAC (cationic) surfactant stabilized water-carbon nanotube nanofluid for drag reduction in a closed loop system. The effectiveness of surfactant as a drag reducing agent has been documented in the open literature [241,242]. In case of crude oil pipeline, drag reducing agents such as surfactant helps in reducing pumping cost by reducing energy loss due to friction. The performance of surfactant as drag reducing agent in a channel flow is attributed to viscoelasticity of solution, structure of micelles and turbulence in flow [241,242].

9. Conclusion and future direction

Favourable properties of nanofluid such as thermal conductivity, viscosity, and surface tension etc. compared to basefluid are beneficial in improving the system performance of several applications. However, one of the critical factors limiting widespread use of nanofluids is its stability. The effectiveness of nanofluid reduces with time due to its instability. The present article reviews several aspects related to nanofluid stability i.e. classification of nanofluids, synthesis methods considering enhanced stability, mechanism responsible for nanofluid stability, different nanofluid stabilization techniques and stability evaluation methods. Specific attention is given on effects of operating conditions for nanofluid stability in several practical applications. Overall, this review focuses on addressing the issues of nanofluid stability from its application perspective starting from the synthesis to operational stage.

The operational conditions of nanofluid i.e. temperature, salinity, composition, shear rate, confinement, external magnetic field etc. can influence its stability. The selection of nanofluid and its preparation method should be decided based on the nature of application and stability consideration. More extensive studies on hybrid stabilization approach i.e. combination of different mechanical and chemical methods should be carried out for enhancing the stability of nanofluid at different operating conditions. Summary of different stability enhancement approaches reviewed in this manuscript can be useful for improving the usability of nanofluid in more number of applications.

Nanofluid stability analysis from operational perspective is one of the important factors for its successful implementation. Systematic studies need to be performed to standardize the effect of operating parameters (high temperature, high pressure, salinity, magnetic field, electrical field, confinement, and shear rate etc.) on nanofluid stability. Compatibility between basefluid and nanoparticle is crucial for achieving longer stability without the need of additional stabilizer. Hydrophilic nanoparticles (metal oxide) are easily dispersed in polar solvent whereas hydrophobic nanoparticles (graphene, carbon nanotube) are compatible in non-polar solvent. From chemical stabilization view point, electrostatic and steric stabilization techniques have been extensively investigated in literature compared to electrosteric stabilization. More studies on electrosteric stabilization technique should be carried out to improve the long term stability and application of nanofluids. Hybrid nanofluids have superior physical characteristics compared to other nanofluids. However, limited study on stability of hybrid nanofluid is available in literature. Further investigation on stability aspects of hybrid nanofluid will enhance its potential for industrial applications. From heat transfer view point, consideration of fouling factor, pressure drop and friction factor should be considered in addition to thermal properties under different operating conditions in heat pipe, heat exchanger, thermosyphon, and microchannel. More studies are also warranted on the effect of flow rate (Re) and particle concentration prior to the application of different nanofluid in heat transfer application. Because, high particle concentration and flow rate can increase pressure drop and fouling effect. The properties of substrate influence the stability of nanofluids in microfluidic applications due to wall effect which require more systematic investigation. Similarly, the porous media properties influence the stability aspects of nanofluids and further investigation is required in design of nanofluids for porous media applications where wall/confinement effect is significant. The design of nanofluids should also be standardized for drag reduction application using systematic study. Oil based nanofluid has superior friction-reduction characteristics due to formation of thick film layer (high viscosity) between two surfaces and low evaporative nature compared to water based nanofluid. Lubrication effect of nanofluid is more prominent for rough surfaces. Limited studies on techno-economic performance of nanofluid are available in open literature considering stability. There are limited studies on stability of nanofluid at high pressure which has relevance in enhanced oil recovery and hydrate formation applications. There are also limited studies on use of graphene quantum dot as a nanoparticle and stabilizer for nanofluid applications. More studies on quantum dot as a potential nanoparticle may enhance the usability of nanofluid for industrial application. Overall, more systematic study on design of nanofluid for specific applications should be carried out from stability perspective. Authors hope that this review will bring the spotlight on the issues related to nanofluid stability and challenges associated with its industrial viability in wider applications. Nanofluid offers significant future scope for use in diverse range of applications.

Declaration of Competing Interest

The authors declare that they have no known competing financial interests or personal relationships that could have appeared to influence the work reported in this paper.

Appendix A. Supplementary data

Supplementary data to this article can be found online at https://doi.org/10.1016/j.applthermaleng.2020.115259.

References

[1] S. Chakraborty, I. Sarkar, A. Ashok, I. Sengupta, S.K. Pal, S. Chakraborty, Synthesis of Cu-Al LDH nanofluid and its application in spray cooling heat transfer of a hot steel plate, Powder Technol. 335 (2018) 285–300.
[2] K. Wusiman, H. Jeong, K. Tulugan, H. Afrianto, H. Chung, Thermal performance of multi-walled carbon nanotubes (MWCNTs) in aqueous suspensions with surfactants SDBS and SDS, Int. Commun. Heat Mass Transfer 41 (2013) 28–33.
[3] A. Indhuja, K.S. Suganthi, S. Manikandan, K.S. Rajan, Viscosity and thermal conductivity of dispersions of gum arabic capped MWCNT in water: influence of MWCNT concentration and temperature, J. Taiwan Inst. Chem. Eng. 44 (2013) 474–479.
[4] W. Yu, H. Xie, L. Chen, Y. Li, Enhancement of thermal conductivity of kerosene-based Fe3O4 nanofluids prepared via phase-transfer method, Colloids Surf., A 355 (2010) 109–113.
[5] D. Li, B. Hong, W. Fang, Y. Guo, R. Lin, Preparation of well-dispersed silver nanoparticles for oil-based nanofluids, Ind. Eng. Chem. Res. 49 (2010) 1697–1702.
[6] Y. Xuan, Q. Li, Heat transfer enhancement of nanofluids, Int. J. Heat Fluid Flow 21 (2000) 58–64.
[7] M.E. Nakhchi, J.A. Esfahani, Cu-water nanofluid flow and heat transfer in a heat exchanger tube equipped with cross-cut twisted tape, Powder Technol. 339 (2018) 985–994.
[8] Yanuar, S. Mau, K.T. Waskito, O.A. Putra, R. Hanif, Drag reduction of alumina nanofluid in spiral pipe with turbulent flow conditions, AIP Conf. Proc. 1826 (2017) 020021.
[9] B.A. Suleimanov, F.S. Ismailov, E.F. Veliyev, Nanofluid for enhanced oil recovery, J. Petrol. Sci. Eng. 78 (2011) 431–437.
[10] H. Zhang, A. Nikolov, D. Wasan, Enhanced oil recovery (EOR) using nanoparticle dispersions: underlying mechanism and imbibition experiments, Energy Fuels 28 (2014) 3002–3009.

[11] W. Yu, H. Xie, A review on nanofluids: preparation, stability mechanisms, and applications, J. Nanomater. 2012 (2012) 17.
[12] M. Khoshvaght-Aliabadi, S. Pazdar, O. Sartipzadeh, Experimental investigation of water based nanofluid containing copper nanoparticles across helical microtubes, Int. Commun. Heat Mass Transfer 70 (2016) 84–92.
[13] W. Yu, H. Xie, W. Chen, Experimental investigation on thermal conductivity of nanofluids containing graphene oxide nanosheets, J. Appl. Phys. 107 (2010) 094317.
[14] A. Naddaf, S. Zeinali Heris, Experimental study on thermal conductivity and electrical conductivity of diesel oil-based nanofluids of graphene nanoplatelets and carbon nanotubes, Int. Commun. Heat Mass Transfer 95 (2018) 116–122.
[15] E. Sadeghinezhad, M. Mehrali, R. Saidur, M. Mehrali, S. Tahan Latibari, A.R. Akhiani, H.S.C. Metselaar, A comprehensive review on graphene nanofluids: recent research, development and applications, Energy Convers. Manage. 111 (2016) 466–487.
[16] H. Xie, H. Lee, W. Youn, M. Choi, Nanofluids containing multiwalled carbon nanotubes and their enhanced thermal conductivities, J. Appl. Phys. 94 (2003) 4967–4971.
[17] M.J. Nine, M. Batmunkh, J.-H. Kim, H.-S. Chung, H.-M. Jeong, Investigation of Al2O3-MWCNTs hybrid dispersion in water and their thermal characterization, J. Nanosci. Nanotechnol. 12 (2012) 4553–4559.
[18] B. Munkhbayar, M.R. Tanshen, J. Jeoun, H. Chung, H. Jeong, Surfactant-free dispersion of silver nanoparticles into MWCNT-aqueous nanofluids prepared by one-step technique and their thermal characteristics, Ceram. Int. 39 (2013) 6415–6425.
[19] L.S. Sundar, M.K. Singh, A.C.M. Sousa, Enhanced heat transfer and friction factor of MWCNT–Fe3O4/water hybrid nanofluids, Int. Commun. Heat Mass Transfer 52 (2014) 73–83.
[20] L.S. Sundar, E. Venkata Ramana, M.P.F. Graça, M.K. Singh, A.C.M. Sousa, Nanodiamond-Fe3O4 nanofluids: preparation and measurement of viscosity, electrical and thermal conductivities, Int. Commun. Heat Mass Transfer 73 (2016) 62–74.
[21] S. Chakraborty, I. Sarkar, K. Haldar, S.K. Pal, S. Chakraborty, Synthesis of Cu–Al layered double hydroxide nanofluid and characterization of its thermal properties, Appl. Clay Sci. 107 (2015) 98–108.
[22] B. LotfizadehDehkordi, S. Kazi, M. Hamdi, A. Ghadimi, E. Sadeghinezhad, H. Metselaar, Investigation of viscosity and thermal conductivity of alumina nanofluids with addition of SDBS, Heat Mass Transf. 49 (2013) 1109–1115.
[23] H.J. Kim, I.C. Bang, J. Onoe, Characteristic stability of bare Au-water nanofluids fabricated by pulsed laser ablation in liquids, Opt. Lasers Eng. 47 (2009) 532–538.
[24] W. Yu, H. Xie, L. Chen, Y. Li, Investigation of thermal conductivity and viscosity of ethylene glycol based ZnO nanofluid, Thermochim Acta 491 (2009) 92–96.
[25] E. Salari, S.M. Peyghambarzadeh, M.M. Sarafraz, F. Hormozi, V. Nikkhah, Thermal behavior of aqueous iron oxide nano-fluid as a coolant on a flat disc heater under the pool boiling condition, Heat Mass Transf. 53 (2016) 265–275.
[26] C. Pang, J.-Y. Jung, J.W. Lee, Y.T. Kang, Thermal conductivity measurement of methanol-based nanofluids with Al2O3 and SiO2 nanoparticles, Int. J. Heat Mass Transf. 55 (2012) 5597–5602.
[27] V. Nikkhah, M.M. Sarafraz, F. Hormozi, S.M. Peyghambarzadeh, Particulate fouling of CuO–water nanofluid at isothermal diffusive condition inside the conventional heat exchanger-experimental and modeling, Exp. Therm Fluid Sci. 60 (2015) 83–95.
[28] M.M. Sarafraz, F. Hormozi, Convective boiling and particulate fouling of stabilized CuO-ethylene glycol nanofluids inside the annular heat exchanger, Int. Commun. Heat Mass Transfer 53 (2014) 116–123.
[29] M. Kamalgharibi, F. Hormozi, S.A.H. Zamzamian, M.M. Sarafraz, Experimental studies on the stability of CuO nanoparticles dispersed in different base fluids: influence of stirring, sonication and surface active agents, Heat Mass Transf. 52 (2015) 55–62.
[30] M.M. Sarafraz, F. Hormozi, S.M. Peyghambarzadeh, Role of nanofluid fouling on thermal performance of a thermosyphon: are nanofluids reliable working fluid? Appl. Therm. Eng. 82 (2015) 212–224.
[31] E. Salari, S.M. Peyghambarzadeh, M.M. Sarafraz, F. Hormozi, Boiling thermal performance of TiO2 aqueous nanofluids as a coolant on a disc copper block, Periodica Polytech., Chem. Eng. 60 (2015) 106–122.
[32] S. Chakraborty, I. Sarkar, D.K. Behera, S.K. Pal, S. Chakraborty, Experimental investigation on the effect of dispersant addition on thermal and rheological characteristics of TiO2 nanofluid, Powder Technol. 307 (2017) 10–24.
[33] A. Ghozatloo, M. Shariaty-Niasar, A.M. Rashidi, Preparation of nanofluids from functionalized Graphene by new alkaline method and study on the thermal conductivity and stability, Int. Commun. Heat Mass Transfer 42 (2013) 89–94.
[34] M.M. Sarafraz, M.R. Safaei, Z. Tian, M. Goodarzi, E.P. Bandarra Filho, M. Arjomandi, Thermal assessment of nano-particulate graphene-water/ethylene glycol (WEG 60: 40) nano-suspension in a compact heat exchanger, Energies 12 (2019) 1929.
[35] M.M. Sarafraz, F. Hormozi, V. Nikkhah, Thermal performance of a counter-current double pipe heat exchanger working with COOH-CNT/water nanofluids, Exp. Therm Fluid Sci. 78 (2016) 41–49.
[36] S. Chakraborty, I. Sarkar, A. Ashok, I. Sengupta, S.K. Pal, S. Chakraborty, Thermophysical properties of Cu-Zn-Al LDH nanofluid and its application in spray cooling, Appl. Therm. Eng. 141 (2018) 339–351.
[37] S. Chakraborty, I. Sengupta, I. Sarkar, S.K. Pal, S. Chakraborty, Effect of surfactant on thermo-physical properties and spray cooling heat transfer performance of Cu-Zn-Al LDH nanofluid, Appl. Clay Sci. 168 (2019) 43–55.
[38] Y. Li, J.E. Zhou, S. Tung, E. Schneider, S. Xi, A review on development of nanofluid preparation and characterization, Powder Technol. 196 (2009) 89–101.
[39] H. Akoh, Y. Tsukasaki, S. Yatsuya, A. Tasaki, Magnetic properties of ferromagnetic ultrafine particles prepared by vacuum evaporation on running oil substrate, J. Cryst. Growth 45 (1978) 495–500.
[40] C.H. Lo, T.T. Tsung, L.C. Chen, Shape-controlled synthesis of Cu-based nanofluid using submerged arc nanoparticle synthesis system (SANSS), J. Cryst. Growth 277 (2005) 636–642.
[41] H.T. Zhu, Y.S. Lin, Y.S. Yin, A novel one-step chemical method for preparation of copper nanofluids, J. Colloid Interface Sci. 277 (2004) 100–103.
[42] A.K. Singh, V.S. Raykar, Microwave synthesis of silver nanofluids with polyvinylpyrrolidone (PVP) and their transport properties, Colloid Polym. Sci. 286 (2008) 1667–1673.
[43] W. Yu, H. Xie, X. Wang, X. Wang, Highly efficient method for preparing homogeneous and stable colloids containing graphene oxide, Nanoscale Res. Lett. 6 (2010) 47.
[44] S. Ayyappan, R.S. Gopalan, G.N. Subbanna, C.N.R. Rao, Nanoparticles of Ag, Au, Pd, and Cu produced by alcohol reduction of the salts, J. Mater. Res. 12 (2011) 398–401.
[45] K.Y. Leong, K.Z. Ku Ahmad, H.C. Ong, M.J. Ghazali, A. Baharum, Synthesis and thermal conductivity characteristic of hybrid nanofluids – A review, Renew. Sustain. Energy Rev. 75 (2017) 868–878.
[46] G. Xia, H. Jiang, R. Liu, Y. Zhai, Effects of surfactant on the stability and thermal conductivity of Al2O3/de-ionized water nanofluids, Int. J. Therm. Sci. 84 (2014) 118–124.
[47] X.J. Wang, D.S. Zhu, S. Yang, Investigation of pH and SDBS on enhancement of thermal conductivity in nanofluids, Chem. Phys. Lett. 470 (2009) 107–111.
[48] L.S. Sundar, M.K. Singh, A.C.M. Sousa, Thermal conductivity of ethylene glycol and water mixture based Fe3O4 nanofluid, Int. Commun. Heat Mass Transfer 49 (2013) 17–24.
[49] R.G. Harrison, P. Todd, S.R. Rudge, D.P. Petrides, Bioseparations Science and Engineering, Oxford University Press, 2015.
[50] W. Chamsa-Ard, S. Brundavanam, C.C. Fung, D. Fawcett, G. Poinern, Nanofluid types, their synthesis, properties and incorporation in direct solar thermal collectors: a review, Nanomaterials (Basel, Switzerland) 7 (2017) 131.
[51] A. Ghadimi, R. Saidur, H.S.C. Metselaar, A review of nanofluid stability properties and characterization in stationary conditions, Int. J. Heat Mass Transf. 54 (2011) 4051–4068.
[52] D.F. Swinehart, The Beer-Lambert law, J. Chem. Educ. 39 (1962) 333.
[53] N. Ali, J.A. Teixeira, A. Addali, A review on nanofluids: fabrication, stability, and thermophysical properties, J. Nanomater. 2018 (2018) 33.
[54] D.W. Oh, A. Jain, J.K. Eaton, K. Goodson, J. Sik Lee, Thermal conductivity measurement and sedimentation detection of aluminum oxide nanofluids by using the 3ω method, Int. J. Heat Fluid Flow 29 (2008) 1456–1461.
[55] R. Prasher, W. Evans, P. Meakin, J. Fish, P. Phelan, P. Keblinski, Effect of aggregation on thermal conduction in colloidal nanofluids, Appl. Phys. Lett. 89 (2006) 143119.
[56] N.R. Karthikeyan, J. Philip, B. Raj, Effect of clustering on the thermal conductivity of nanofluids, Mater. Chem. Phys. 109 (2008) 50–55.
[57] S. Bhattacharjee, DLS and zeta potential – What they are and what they are not? J. Control. Release 235 (2016) 337–351.
[58] M. Kole, T.K. Dey, Effect of aggregation on the viscosity of copper oxide–gear oil nanofluids, Int. J. Therm. Sci. 50 (2011) 1741–1747.
[59] R. Sadeghi, S.G. Etemad, E. Keshavarzi, M. Haghshenasfard, Investigation of alumina nanofluid stability by UV–vis spectrum, Microfluid. Nanofluid. 18 (2015) 1023–1030.
[60] D.A. Walker, B. Kowalczyk, M.O. de la Cruz, B.A. Grzybowski, Electrostatics at the nanoscale, Nanoscale 3 (2011) 1316–1344.
[61] N. Bell, D. Dimos, Calculation of hamaker constants in nonaqueous fluid media, MRS Proc. 624 (2011) 275.
[62] C. Rodríguez-Abreu, Chapter 1 - nanocolloids: some basic concepts and principles of their stabilization, in: M.S. Domínguez, C.R. Abreu (Eds.), Nanocolloids, Elsevier, Amsterdam, 2016, pp. 1–36.
[63] E.M. Hotze, T. Phenrat, G.V. Lowry, Nanoparticle aggregation: challenges to understanding transport and reactivity in the environment, J. Environ. Qual. 39 (2010) 1909–1924.
[64] D.C. Gregg, Practical organic chemistry (Vogel, Arthur I.), J. Chem. Educ. 29 (1952) 320.
[65] P.I.P. Soares, C.A.T. Laia, A. Carvalho, L.C.J. Pereira, J.T. Coutinho, I.M.M. Ferreira, C.M.M. Novo, J.P. Borges, Iron oxide nanoparticles stabilized with a bilayer of oleic acid for magnetic hyperthermia and MRI applications, Appl. Surf. Sci. 383 (2016) 240–247.
[66] S. Umar, F. Sulaiman, N. Abdullah, S.N. Mohamad, Investigation of the effect of pH adjustment on the stability of nanofluid, AIP Conf. Proc. 2031 (2018) 020031.
[67] S.K. Babita, S.M. Sharma, Gupta, Preparation and evaluation of stable nanofluids for heat transfer application: a review, Exp. Therm Fluid Sci. 79 (2016) 202–212.
[68] Y.T. He, J. Wan, T. Tokunaga, Kinetic stability of hematite nanoparticles: the effect of particle sizes, J. Nanopart. Res. 10 (2008) 321–332.
[69] H.J. Kim, S.H. Lee, J.H. Lee, S.P. Jang, Effect of particle shape on suspension stability and thermal conductivities of water-based bohemite alumina nanofluids, Energy 90 (2015) 1290–1297.
[70] S.N.D. Santos, E.S. Bernardes, R. Santos-Oliveira, Chapter 18 - Nanoradiopharmaceuticals in current molecular medicine, in: A. Barhoum, A.S. Hamdy Makhlouf (Eds.), Fundamentals of Nanoparticles, Elsevier, 2018, pp. 553–569.
[71] M.J. Vold, Van der Waals' attraction between anisometric particles, J. Colloid Sci. 9 (1954) 451–459.
[72] T. Vitez, P. Trávníček, Study of settling velocity of sand particles located in

wastewater treatment plant, Acta Univ. Agric. Silvicult. Mendelianae Brunensis 59 (2011) 249–254.
[73] K.S. Hong, T.-K. Hong, H.-S. Yang, Thermal conductivity of Fe nanofluids depending on the cluster size of nanoparticles, Appl. Phys. Lett. 88 (2006) 031901.
[74] I.M. Mahbubul, E.B. Elcioglu, R. Saidur, M.A. Amalina, Optimization of ultrasonication period for better dispersion and stability of TiO2–water nanofluid, Ultrason. Sonochem. 37 (2017) 360–367.
[75] J. Shah, M. Ranjan, S.K. Gupta, Y. Sonvane, Ultrasonication effect on thermophysical properties of Al2O3 nanofluids, AIP Conf. Proc. 1951 (2018) 020008.
[76] V.S. Nguyen, D. Rouxel, R. Hadji, B. Vincent, Y. Fort, Effect of ultrasonication and dispersion stability on the cluster size of alumina nanoscale particles in aqueous solutions, Ultrason. Sonochem. 18 (2011) 382–388.
[77] A. Amrollahi, A. Hamidi, A. Rashidi, The effects of temperature, volume fraction and vibration time on the thermo-physical properties of a carbon nanotube suspension (carbon nanofluid), Nanotechnology 19 (2008) 315701.
[78] A. Shahsavar, M.R. Salimpour, M. Saghafian, M.B. Shafii, An experimental study on the effect of ultrasonication on thermal conductivity of ferrofluid loaded with carbon nanotubes, Thermochim Acta 617 (2015) 102–110.
[79] R. Sadri, G. Ahmadi, H. Togun, M. Dahari, S.N. Kazi, E. Sadeghinezhad, N. Zubir, An experimental study on thermal conductivity and viscosity of nanofluids containing carbon nanotubes, Nanoscale Res. Lett. 9 (2014) 151.
[80] H.J. Chen, D. Wen, Ultrasonic-aided fabrication of gold nanofluids, Nanoscale Res. Lett. 6 (2011) 198.
[81] J. Boopathy, R. Pari, M. Kavitha, P.C. Angelo, Preparation of nano fluids by mechanical method, AIP Conf. Proc. 1461 (2012) 218–221.
[82] S. Mukherjee, P.C. Mishra, P. Chaudhuri, Stability of heat transfer nanofluids - a review, ChemBioEng Rev. 5 (2018) 312–333.
[83] S.U. Ilyas, R. Pendyala, N. Marneni, Stability of nanofluids, in: V.S. Korada, N. Hisham, B. Hamid (Eds.), Engineering Applications of Nanotechnology: From Energy to Drug Delivery, Springer International Publishing, Cham, 2017, pp. 1–31.
[84] D. Dey, P. Kumar, S. Samantaray, A review of nanofluid preparation, stability, and thermo-physical properties, Heat Transfer: Asian Res. 46 (2017) 1413–1442.
[85] L. Fedele, L. Colla, S. Bobbo, S. Barison, F. Agresti, Experimental stability analysis of different water-based nanofluids, Nanoscale Res. Lett. 6 (2011) 300.
[86] M. Drzazga, A. Gierczycki, G. Dzido, M. Lemanowicz, Influence of nonionic surfactant addition on drag reduction of water based nanofluid in a small diameter pipe, Chin. J. Chem. Eng. 21 (2013) 104–108.
[87] B.M. Paramashivaiah, C.R. Rajashekhar, Studies on effect of various surfactants on stable dispersion of graphene nano particles in simarouba biodiesel, IOP Conf. Ser.: Mater. Sci. Eng. 149 (2016) 012083.
[88] H. Vatanparast, F. Shahabi, A. Bahramian, A. Javadi, R. Miller, The role of electrostatic repulsion on increasing surface activity of anionic surfactants in the presence of hydrophilic silica nanoparticles, Sci. Rep. 8 (2018) 7251.
[89] A. Amiri, M. Naraghi, G. Ahmadi, M. Soleymaniha, M. Shanbedi, A review on liquid-phase exfoliation for scalable production of pure graphene, wrinkled, crumpled and functionalized graphene and challenges, FlatChem 8 (2018) 40–71.
[90] M. Lotya, P.J. King, U. Khan, S. De, J.N. Coleman, High-concentration, surfactant-stabilized graphene dispersions, ACS Nano 4 (2010) 3155–3162.
[91] T. Hasan, F. Torrisi, Z. Sun, D. Popa, V. Nicolosi, G. Privitera, F. Bonaccorso, A.C. Ferrari, Solution-phase exfoliation of graphite for ultrafast photonics, Physica Status Solidi (b) 247 (2010) 2953–2957.
[92] A. Schlierf, H. Yang, E. Gebremedhn, E. Treossi, L. Ortolani, L. Chen, A. Minoia, V. Morandi, P. Samorì, C. Casiraghi, D. Beljonne, V. Palermo, Nanoscale insight into the exfoliation mechanism of graphene with organic dyes: effect of charge, dipole and molecular structure, Nanoscale 5 (2013) 4205–4216.
[93] D. Parviz, S. Das, H.S.T. Ahmed, F. Irin, S. Bhattacharia, M.J. Green, Dispersions of non-covalently functionalized graphene with minimal stabilizer, ACS Nano 6 (2012) 8857–8867.
[94] J.-H. Jang, D. Rangappa, Y.-U. Kwon, I. Honma, Direct preparation of 1-PSA modified graphene nanosheets by supercritical fluidic exfoliation and its electrochemical properties, J. Mater. Chem. 21 (2011) 3462–3466.
[95] X. An, T. Simmons, R. Shah, C. Wolfe, K.M. Lewis, M. Washington, S.K. Nayak, S. Talapatra, S. Kar, Stable aqueous dispersions of noncovalently functionalized graphene from graphite and their multifunctional high-performance applications, Nano Lett. 10 (2010) 4295–4301.
[96] M. Zhang, R.R. Parajuli, D. Mastrogiovanni, B. Dai, P. Lo, W. Cheung, R. Brukh, P.L. Chiu, T. Zhou, Z. Liu, E. Garfunkel, H. He, Production of graphene sheets by direct dispersion with aromatic healing agents, Small 6 (2010) 1100–1107.
[97] A. Ghosh, K.V. Rao, S.J. George, C.N.R. Rao, Noncovalent functionalization, exfoliation, and solubilization of graphene in water by employing a fluorescent coronene carboxylate, Chem. – A Eur. J. 16 (2010) 2700–2704.
[98] J.M. Englert, J. Röhrl, C.D. Schmidt, R. Graupner, M. Hundhausen, F. Hauke, A. Hirsch, Soluble graphene: generation of aqueous graphene solutions aided by a perylenebisimide-based bolaamphiphile, Adv. Mater. 21 (2009) 4265–4269.
[99] S.S.J. Aravind, P. Baskar, T.T. Baby, R.K. Sabareesh, S. Das, S. Ramaprabhu, Investigation of structural stability, dispersion, viscosity, and conductive heat transfer properties of functionalized carbon nanotube based nanofluids, J. Phys. Chem. C 115 (2011) 16737–16744.
[100] H.S. Xue, J.R. Fan, Y.C. Hu, R.H. Hong, K.F. Cen, The interface effect of carbon nanotube suspension on the thermal performance of a two-phase closed thermosyphon, J. Appl. Phys. 100 (2006) 104909.
[101] A. Amiri, R. Sadri, M. Shanbedi, G. Ahmadi, B.T. Chew, S.N. Kazi, M. Dahari, Performance dependence of thermosyphon on the functionalization approaches: an experimental study on thermo-physical properties of graphene nanoplatelet-based water nanofluids, Energy Convers. Manage. 92 (2015) 322–330.
[102] A. Amiri, M. Shanbedi, H. Amiri, S.Z. Heris, S.N. Kazi, B.T. Chew, H. Eshghi, Pool boiling heat transfer of CNT/water nanofluids, Appl. Therm. Eng. 71 (2014) 450–459.
[103] K.J. Park, D. Jung, Boiling heat transfer enhancement with carbon nanotubes for refrigerants used in building air-conditioning, Energy Build. 39 (2007) 1061–1064.
[104] M.F. Islam, E. Rojas, D.M. Bergey, A.T. Johnson, A.G. Yodh, High weight fraction surfactant solubilization of single-wall carbon nanotubes in water, Nano Lett. 3 (2003) 269–273.
[105] M.J. Assael, C.F. Chen, I. Metaxa, W.A. Wakeham, Thermal conductivity of suspensions of carbon nanotubes in water, Int. J. Thermophys. 25 (2004) 971–985.
[106] M. Shanbedi, S. Zeinali Heris, M. Baniadam, A. Amiri, The effect of multi-walled carbon nanotube/water nanofluid on thermal performance of a two-phase closed thermosyphon, Exp. Heat Transfer 26 (2013) 26–40.
[107] M.N.A.W.M. Yazid, N.A.C. Sidik, R. Mamat, G. Najafi, A review of the impact of preparation on stability of carbon nanotube nanofluids, Int. Commun. Heat Mass Transfer 78 (2016) 253–263.
[108] A. Amiri, M. Shanbedi, B.T. Chew, S.N. Kazi, K.H. Solangi, Toward improved engine performance with crumpled nitrogen-doped graphene based water—ethylene glycol coolant, Chem. Eng. J. 289 (2016) 583–595.
[109] A. Amiri, M. Shanbedi, H. Dashti, Thermophysical and rheological properties of water-based graphene quantum dots nanofluids, J. Taiwan Inst. Chem. Eng. 76 (2017) 132–140.
[110] M. Soleymaniha, A. Amiri, M. Shanbedi, B.T. Chew, S. Wongwises, Water-based graphene quantum dots dispersion as a high-performance long-term stable nanofluid for two-phased closed thermosyphons, Int. Commun. Heat Mass Transfer 95 (2018) 147–154.
[111] E. Ettefaghi, B. Ghobadian, A. Rashidi, G. Najafi, M.H. Khoshtaghaza, S. Pourhashem, Preparation and investigation of the heat transfer properties of a novel nanofluid based on graphene quantum dots, Energy Convers. Manage. 153 (2017) 215–223.
[112] P. He, J. Sun, S. Tian, S. Yang, S. Ding, G. Ding, X. Xie, M. Jiang, Processable aqueous dispersions of graphene stabilized by graphene quantum dots, Chem. Mater. 27 (2015) 218–226.
[113] D. Lee, J.-W. Kim, B.G. Kim, A new parameter to control heat transport in nanofluids: surface charge state of the particle in suspension, J. Phys. Chem. B 110 (2006) 4323–4328.
[114] X. Wei, H. Zhu, T. Kong, L. Wang, Synthesis and thermal conductivity of Cu2O nanofluids, Int. J. Heat Mass Transf. 52 (2009) 4371–4374.
[115] X.F. Li, D.S. Zhu, X.J. Wang, N. Wang, J.W. Gao, H. Li, Thermal conductivity enhancement dependent pH and chemical surfactant for Cu-H2O nanofluids, Thermochim Acta 469 (2008) 98–103.
[116] D. Wen, Y. Ding, Experimental investigation into the pool boiling heat transfer of aqueous based γ-alumina nanofluids, J. Nanopart. Res. 7 (2005) 265–274.
[117] K.A. Wepasnick, B.A. Smith, J.L. Bitter, D. Howard Fairbrother, Chemical and structural characterization of carbon nanotube surfaces, Anal. Bioanal. Chem. 396 (2010) 1003–1014.
[118] B. Smith, K. Wepasnick, K.E. Schrote, A.R. Bertele, W.P. Ball, C. O'Melia, D.H. Fairbrother, Colloidal properties of aqueous suspensions of acid-treated, multi-walled carbon nanotubes, Environ. Sci. Technol. 43 (2009) 819–825.
[119] M. Liu, Y. Yang, T. Zhu, Z. Liu, Chemical modification of single-walled carbon nanotubes with peroxytrifluoroacetic acid, Carbon 43 (2005) 1470–1478.
[120] Q. Yu, Y.J. Kim, H. Ma, Nanofluids with plasma treated diamond nanoparticles, Appl. Phys. Lett. 92 (2008) 103111.
[121] K.J. Park, D. Jung, S.E. Shim, Nucleate boiling heat transfer in aqueous solutions with carbon nanotubes up to critical heat fluxes, Int. J. Multiph. Flow 35 (2009) 525–532.
[122] E. Piacenza, A. Presentato, R.J. Turner, Stability of biogenic metal(loid) nanomaterials related to the colloidal stabilization theory of chemical nanostructures, Crit. Rev. Biotechnol. 38 (2018) 1137–1156.
[123] G. Cao, Nanostructures and Nanomaterials, Published By Imperial College Press and distributed by World Scientific Publishing Co., 2004.
[124] J.Y. Choi, J.Y. Yoo, H.S. Kwak, B. Uk Nam, J. Lee, Role of polymeric stabilizers for drug nanocrystal dispersions, Curr. Appl Phys. 5 (2005) 472–474.
[125] B. Derjaguin, L. Landau, Theory of the stability of strongly charged lyophobic sols and of the adhesion of strongly charged particles in solutions of electrolytes, Prog. Surf. Sci. 43 (1993) 30–59.
[126] E.M.V. Hoek, G.K. Agarwal, Extended DLVO interactions between spherical particles and rough surfaces, J. Colloid Interface Sci. 298 (2006) 50–58.
[127] H. Zecha, Stabilization of colloidal dispersions by polymer adsorption. Von TATSUO SATO und RICHARD RUCH. Surfactant Science Series. New York/Basel: Marcel Dekker Inc. 1980. 155 S., 46 Abb., 302 Lit. SFr. 58.—, Acta Polymerica 32 (1981) 582.
[128] R. Bandyopadhyaya, E. Nativ-Roth, O. Regev, R. Yerushalmi-Rozen, Stabilization of individual carbon nanotubes in aqueous solutions, Nano Lett. 2 (2002) 25–28.
[129] M. Sahooli, S. Sabbaghi, M. Shariaty Niassar, Preparation of CuO/water nanofluids using polyvinylpyrolidone and a survey on its stability and thermal conductivity, Int. J. Nanosci. Nanotechnol. 8 (2012) 27–34.
[130] M. Shanbedi, S. Zeinali Heris, A. Maskooki, Experimental investigation of stability and thermophysical properties of carbon nanotubes suspension in the presence of different surfactants, J. Therm. Anal. Calorim. 120 (2015) 1193–1201.
[131] Q.Y. Tang, S. Ismathullakhan, Y.C. Chanl, N.B. Wong, R. Cheung, Study of the dispersion and electrical properties of carbon nanotubes treated by surfactants in dimethylacetamide, J. Nanosci. Nanotechnol. 10 (2010) 4967–4974.
[132] Y. Hwang, J.K. Lee, J.K. Lee, Y.M. Jeong, S.I. Cheong, Y.C. Ahn, S.H. Kim, Production and dispersion stability of nanoparticles in nanofluids, Powder Technol. 186 (2008) 145–153.

[133] H.S. Kim, W.I. Park, M. Kang, H.J. Jin, Multiple light scattering measurement and stability analysis of aqueous carbon nanotube dispersions, J. Phys. Chem. Solids 69 (2008) 1209–1212.
[134] E. González, M. Paulis, M.J. Barandiaran, Effect of controlled length acrylic acid-based electrosteric stabilizers on latex film properties, Eur. Polym. J. 59 (2014) 122–128.
[135] K. Manojkumar, A. Sivaramakrishna, K. Vijayakrishna, A short review on stable metal nanoparticles using ionic liquids, supported ionic liquids, and poly(ionic liquids), J. Nanopart. Res. 18 (2016) 103.
[136] H.J. Kong, S.G. Bike, V.C. Li, Electrosteric stabilization of concentrated cement suspensions imparted by a strong anionic polyelectrolyte and a non-ionic polymer, Cem. Concr. Res. 36 (2006) 842–850.
[137] V. Srinivas, C.V.K.N.S.N. Moorthy, V. Dedeepya, P.V. Manikanta, V. Satish, Nanofluids with CNTs for automotive applications, Heat Mass Transf. 52 (2016) 701–712.
[138] G.S. Wu, J.K. Yang, S.L. Ge, Y.J. Wang, M.H. Chen, Y.F. Chen, Thermal conductivity measurement for carbon-nanotube suspensions with 3ω method, Adv. Mater. Res. 60–61 (2009) 394–398.
[139] J. Yu, N. Grossiord, C.E. Koning, J. Loos, Controlling the dispersion of multi-wall carbon nanotubes in aqueous surfactant solution, Carbon 45 (2007) 618–623.
[140] X. Li, D. Zhu, X. Wang, Evaluation on dispersion behavior of the aqueous copper nano-suspensions, J. Colloid Interface Sci. 310 (2007) 456–463.
[141] H. Sandhu, G. Dasaroju, M. Singh, Experimental study on stability of different nanofluids by using different nanoparticles and basefluids, 4th Thermal and Fluids Engineering Conference, 2019, p. 27991.
[142] R. Choudhary, D. Khurana, A. Kumar, S. Subudhi, Stability analysis of Al2O3/water nanofluids, J. Exp. Nanosci. 12 (2017) 140–151.
[143] S. Mo, Y. Chen, L. Jia, X. Luo, Investigation on crystallization of TiO2–water nanofluids and deionized water, Appl. Energy 93 (2012) 65–70.
[144] A. Ghadimi, I.H. Metselaar, The influence of surfactant and ultrasonic processing on improvement of stability, thermal conductivity and viscosity of Titania nanofluid, Exp. Therm Fluid Sci. 51 (2013) 1–9.
[145] H.G. Bagaria, B.M. Neilson, A.J. Worthen, Z. Xue, K.Y. Yoon, V. Cheng, J.H. Lee, S. Velagala, C. Huh, S.L. Bryant, C.W. Bielawski, K.P. Johnston, Adsorption of iron oxide nanoclusters stabilized with sulfonated copolymers on silica in concentrated NaCl and CaCl2 brine, J. Colloid Interface Sci. 398 (2013) 217–226.
[146] M. Iqbal, B.A. Lyon, E.E. Ureña-Benavides, E. Moaseri, Y. Fei, C. McFadden, K.J. Javier, C.J. Ellison, K.D. Pennell, K.P. Johnston, High temperature stability and low adsorption of sub-100nm magnetite nanoparticles grafted with sulfonated copolymers on Berea sandstone in high salinity brine, Colloids Surf., A 520 (2017) 257–267.
[147] Y.Y. Song, H.K.D.H. Bhadeshia, D.W. Suh, Stability of stainless-steel nanoparticle and water mixtures, Powder Technol. 272 (2015) 34–44.
[148] S. Mitra, S.K. Saha, S. Chakraborty, S. Das, Study on boiling heat transfer of water–TiO2 and water–MWCNT nanofluids based laminar jet impingement on heated steel surface, Appl. Therm. Eng. 37 (2012) 353–359.
[149] M.R. Sohel, R. Saidur, S.S. Khaleduzzaman, T.A. Ibrahim, Cooling performance investigation of electronics cooling system using Al2O3–H2O nanofluid, Int. Commun. Heat Mass Transfer 65 (2015) 89–93.
[150] S.S. Khaleduzzaman, M.R. Sohel, R. Saidur, I.M. Mahbubul, I.M. Shahrul, B.A. Akash, J. Selvaraj, Energy and exergy analysis of alumina–water nanofluid for an electronic liquid cooling system, Int. Commun. Heat Mass Transfer 57 (2014) 118–127.
[151] T. Yousefi, F. Veysi, E. Shojaeizadeh, S. Zinadini, An experimental investigation on the effect of Al2O3–H2O nanofluid on the efficiency of flat-plate solar collectors, Renewable Energy 39 (2012) 293–298.
[152] A.J. Moghadam, M. Farzane-Gord, M. Sajadi, M. Hoseyn-Zadeh, Effects of CuO/water nanofluid on the efficiency of a flat-plate solar collector, Exp. Therm Fluid Sci. 58 (2014) 9–14.
[153] V. Ghazanfari, M. Talebi, J. Khorsandi, R. Abdolahi, Thermal–hydraulic modeling of water/Al2O3 nanofluid as the coolant in annular fuels for a typical VVER-1000 core, Prog. Nucl. Energy 87 (2016) 67–73.
[154] H.R. Allahyar, F. Hormozi, B. ZareNezhad, Experimental investigation on the thermal performance of a coiled heat exchanger using a new hybrid nanofluid, Exp. Therm Fluid Sci. 76 (2016) 324–329.
[155] R. Saleh, N. Putra, R.E. Wibowo, W.N. Septiadi, S.P. Prakoso, Titanium dioxide nanofluids for heat transfer applications, Exp. Therm Fluid Sci. 52 (2014) 19–29.
[156] P. Yi, A.A. Kayani, A.F. Chrimes, K. Ghorbani, S. Nahavandi, K. Kalantar-zadeh, K. Khoshmanesh, Thermal analysis of nanofluids in microfluidics using an infrared camera, Lab Chip 12 (2012) 2520–2525.
[157] P.H. Chen, D.S. Liou, T.H. Tsai, L.S. Kuo, C.T. Yang, Applications of nanofluids in microfluidic devices, ASME 2008 6th International Conference on Nanochannels, Microchannels, and Minichannels, Vol. ASME 2008 6th International Conference on Nanochannels, Microchannels, and Minichannels, 2008, pp. 1669–1675.
[158] N.A.C. Sidik, M.N.A.W.M. Yazid, R. Mamat, A review on the application of nanofluids in vehicle engine cooling system, Int. Commun. Heat Mass Transfer 68 (2015) 85–90.
[159] K. Li, D. Wang, S. Jiang, Review on enhanced oil recovery by nanofluids, Oil Gas Sci. Technol. – Revue d'IFP Energies nouvelles 73 (2018) 37.
[160] H. ShamsiJazeyi, C.A. Miller, M.S. Wong, J.M. Tour, R. Verduzco, Polymer-coated nanoparticles for enhanced oil recovery, J. Appl. Polym. Sci. 131 (2014) 40576.
[161] N. Sezer, M. Koç, Dispersion stability of CNT and CNT/Metal-based nanofluids, in: 11th International Conference on Thermal Engineering, Vol. 2018, 2018, pp. 1–4.
[162] V.O. Aseyev, H. Tenhu, F.M. Winnik, Temperature dependence of the colloidal stability of neutral amphiphilicpolymers in water, in: A.R. Khokhlov (Ed.), Conformation-Dependent Design of Sequences in Copolymers II, Springer, Berlin Heidelberg, 2006, pp. 1–85.
[163] J. Tavares, S. Coulombe, Dual plasma synthesis and characterization of a stable copper–ethylene glycol nanofluid, Powder Technol. 210 (2011) 132–142.
[164] R.A. Taylor, P.E. Phelan, T.P. Otanicar, C.A. Walker, M. Nguyen, S. Trimble, R. Prasher, Applicability of nanofluids in high flux solar collectors, J. Renewable Sustainable Energy 3 (2011) 023104.
[165] H. Chang, C. Hung Lo, T. Tshih Tsung, Y.Y. Cho, D. Tien, L.C. Chen, C.H. Thai, Temperature effect on the stability of CuO nanofluids based on measured particle distribution, Key Eng. Mater. 295–296 (2005) 51–56.
[166] E. Sani, L. Mercatelli, S. Barison, C. Pagura, F. Agresti, L. Colla, P. Sansoni, Potential of carbon nanohorn-based suspensions for solar thermal collectors, Sol. Energy Mater. Sol. Cells 95 (2011) 2994–3000.
[167] N. Hordy, D. Rabilloud, J.-L. Meunier, S. Coulombe, High temperature and long-term stability of carbon nanotube nanofluids for direct absorption solar thermal collectors, Sol. Energy 105 (2014) 82–90.
[168] M.M. Sarafraz, H. Arya, M. Saeedi, D. Ahmadi, Flow boiling heat transfer to MgO-therminol 66 heat transfer fluid: experimental assessment and correlation development, Appl. Therm. Eng. 138 (2018) 552–562.
[169] M.M. Sarafraz, Thermal performance and viscosity of biologically produced silver/coconut oil nanofluids, Chem. Biochem. Eng. Quart. J. 30 (2017) 489–500.
[170] F.R. Dareh, M. Haghshenasfard, M. Nasr Esfahany, H. Reza Salimi Jazi, An experimental investigation of pool boiling characteristics of alumina-water nanofluid over micro-/nanostructured surfaces, Heat Transfer Eng. 40 (2019) 1691–1708.
[171] N.A.A. Bakar, N. Bachok, N.M. Arifin, I. Pop, Stability analysis on the flow and heat transfer of nanofluid past a stretching/shrinking cylinder with suction effect, Results Phys. 9 (2018) 1335–1344.
[172] J. Lin, H. Yang, A review on the flow instability of nanofluids, Appl. Math. Mech. 40 (2019) 1227–1238.
[173] A. Kanjirakat, R. Sadr, Near-wall velocity profile measurement for nanofluids, AIP Adv. 6 (2016) 015308.
[174] C. Yang, Q. Wang, A. Nakayama, T. Qiu, Effect of temperature jump on forced convective transport of nanofluids in the continuum flow and slip flow regimes, Chem. Eng. Sci. 137 (2015) 730–739.
[175] B.C. Pak, Y.I. Cho, Hydrodynamic and heat transfer study of dispersed fluids with submicron metallic oxide particles, Exp. Heat Transfer 11 (1998) 151–170.
[176] W. Evans, R. Prasher, J. Fish, P. Meakin, P. Phelan, P. Keblinski, Effect of aggregation and interfacial thermal resistance on thermal conductivity of nanocomposites and colloidal nanofluids, Int. J. Heat Mass Transf. 51 (2008) 1431–1438.
[177] D. Wen, G. Lin, S. Vafaei, K. Zhang, Review of nanofluids for heat transfer applications, Particuology 7 (2009) 141–150.
[178] E.V. Timofeeva, A.N. Gavrilov, J.M. McCloskey, Y.V. Tolmachev, S. Sprunt, L.M. Lopatina, J.V. Selinger, Thermal conductivity and particle agglomeration in alumina nanofluids: experiment and theory, Phys. Rev. E 76 (2007) 061203.
[179] B. Wei, C. Zou, X. Li, Experimental investigation on stability and thermal conductivity of diathermic oil based TiO2 nanofluids, Int. J. Heat Mass Transf. 104 (2017) 537–543.
[180] E.B. Haghighi, N. Nikkam, M. Saleemi, M. Behi, S.A. Mirmohammadi, H. Poth, R. Khodabandeh, M.S. Toprak, M. Muhammed, B. Palm, Shelf stability of nanofluids and its effect on thermal conductivity and viscosity, Meas. Sci. Technol. 24 (2013) 105301.
[181] Y. Su, L. Gong, B. Li, Z. Liu, D. Chen, Performance evaluation of nanofluid MQL with vegetable-based oil and ester oil as base fluids in turning, Int. J. Adv. Manuf. Technol. 83 (2016) 2083–2089.
[182] M.A. Sabiha, R.M. Mostafizur, R. Saidur, S. Mekhilef, Experimental investigation on thermo physical properties of single walled carbon nanotube nanofluids, Int. J. Heat Mass Transf. 93 (2016) 862–871.
[183] N. Ahammed, L.G. Asirvatham, S. Wongwises, Effect of volume concentration and temperature on viscosity and surface tension of graphene–water nanofluid for heat transfer applications, J. Therm. Anal. Calorim. 123 (2016) 1399–1409.
[184] F. Duan, D. Kwek, A. Crivoi, Viscosity affected by nanoparticle aggregation in Al2O3-water nanofluids, Nanoscale Res. Lett. 6 (2011) 248.
[185] H. Chen, Y. Ding, C. Tan, Rheological behaviour of nanofluids, New J. Phys. 9 (2007) 367.
[186] B. Aladag, S. Halelfadl, N. Doner, T. Maré, S. Duret, P. Estellé, Experimental investigations of the viscosity of nanofluids at low temperatures, Appl. Energy 97 (2012) 876–880.
[187] M.J. Pastoriza-Gallego, C. Casanova, J.L. Legido, M.M. Piñeiro, CuO in water nanofluid: influence of particle size and polydispersity on volumetric behaviour and viscosity, Fluid Phase Equilib. 300 (2011) 188–196.
[188] J.C. Yang, F.C. Li, W.W. Zhou, Y.R. He, B.C. Jiang, Experimental investigation on the thermal conductivity and shear viscosity of viscoelastic-fluid-based nanofluids, Int. J. Heat Mass Transf. 55 (2012) 3160–3166.
[189] M. Silambarasan, S. Manikandan, K.S. Rajan, Viscosity and thermal conductivity of dispersions of sub-micron TiO2 particles in water prepared by stirred bead milling and ultrasonication, Int. J. Heat Mass Transf. 55 (2012) 7991–8002.
[190] M. Kole, T.K. Dey, Investigation of thermal conductivity, viscosity, and electrical conductivity of graphene based nanofluids, J. Appl. Phys. 113 (2013) 084307.
[191] A.T. Utomo, H. Poth, P.T. Robbins, A.W. Pacek, Experimental and theoretical studies of thermal conductivity, viscosity and heat transfer coefficient of Titania and alumina nanofluids, Int. J. Heat Mass Transf. 55 (2012) 7772–7781.
[192] A.K. Tiwari, P. Ghosh, J. Sarkar, Heat transfer and pressure drop characteristics of CeO2/water nanofluid in plate heat exchanger, Appl. Therm. Eng. 57 (2013) 24–32.
[193] T. Wang, M. Ni, Z. Luo, C. Shou, K. Cen, Viscosity and aggregation structure of nanocolloidal dispersions, Chin. Sci. Bull. 57 (2012) 3644–3651.

[194] M. Moosavi, E.K. Goharshadi, A. Youssefi, Fabrication, characterization, and measurement of some physicochemical properties of ZnO nanofluids, Int. J. Heat Fluid Flow 31 (2010) 599–605.
[195] S.S. Khaleduzzaman, I.M. Mahbubul, I.M. Shahrul, R. Saidur, Effect of particle concentration, temperature and surfactant on surface tension of nanofluids, Int. Commun. Heat Mass Transfer 49 (2013) 110–114.
[196] S. Vafaei, A. Purkayastha, A. Jain, G. Ramanath, T. Borca-Tasciuc, The effect of nanoparticles on the liquid–gas surface tension of Bi2Te3nanofluids, Nanotechnology 20 (2009) 185702.
[197] A. Alirezaie, M.H. Hajmohammad, M.R. Hassani Ahangar, M. Hemmat Esfe, Price-performance evaluation of thermal conductivity enhancement of nanofluids with different particle sizes, Appl. Therm. Eng. 128 (2018) 373–380.
[198] M. Hemmat Esfe, A.A. Abbasian Arani, M. Firouzi, Empirical study and model development of thermal conductivity improvement and assessment of cost and sensitivity of EG-water based SWCNT-ZnO (30%:70%) hybrid nanofluid, J. Mol. Liq. 244 (2017) 252–261.
[199] M. Asfer, S.K. Saroj, P.K. Panigrahi, Retention of ferrofluid aggregates at the target site during magnetic drug targeting, J. Magn. Magn. Mater. 436 (2017) 47–56.
[200] M. Asfer, B. Mehta, A. Kumar, S. Khandekar, P.K. Panigrahi, Effect of magnetic field on laminar convective heat transfer characteristics of ferrofluid flowing through a circular stainless steel tube, Int. J. Heat Fluid Flow 59 (2016) 74–86.
[201] S.K. Saroj, P.K. Panigrahi, Effect of salt concentration (NaCl) on drying pattern of ferrofluid droplets, J. Flow Visual. Image Process. 25 (2018) 245–258.
[202] S.K. Saroj, P.K. Panigrahi, Drying pattern and evaporation dynamics of sessile ferrofluid droplet on a PDMS substrate, Colloids Surf., A 580 (2019) 123672.
[203] B. Fani, A. Abbassi, M. Kalteh, Effect of nanoparticles size on thermal performance of nanofluid in a trapezoidal microchannel-heat-sink, Int. Commun. Heat Mass Transfer 45 (2013) 155–161.
[204] M.M. Sarafraz, B. Yang, O. Pourmehran, M. Arjomandi, R. Ghomashchi, Fluid and heat transfer characteristics of aqueous graphene nanoplatelet (GNP) nanofluid in a microchannel, Int. Commun. Heat Mass Transfer 107 (2019) 24–33.
[205] M. Sarafraz, V. Nikkhah, M. Nakhjavani, A. Arya, Fouling formation and thermal performance of aqueous carbon nanotube nanofluid in a heat sink with rectangular parallel microchannel, Appl. Therm. Eng. 123 (2017) 29–39.
[206] G.D. Xia, R. Liu, J. Wang, M. Du, The characteristics of convective heat transfer in microchannel heat sinks using Al2O3 and TiO2 nanofluids, Int. Commun. Heat Mass Transfer 76 (2016) 256–264.
[207] B. Rimbault, C.T. Nguyen, N. Galanis, Experimental investigation of CuO–water nanofluid flow and heat transfer inside a microchannel heat sink, Int. J. Therm. Sci. 84 (2014) 275–292.
[208] M.D. Byrne, R.A. Hart, A.K. da Silva, Experimental thermal–hydraulic evaluation of CuO nanofluids in microchannels at various concentrations with and without suspension enhancers, Int. J. Heat Mass Transf. 55 (2012) 2684–2691.
[209] B. Moradi, P. Pourafshary, F.J. Farahani, M. Mohammadi, M.A. Emadi, Application of SiO2 nano particles to improve the performance of water alternating gas EOR process, SPE Oil & Gas India Conference and Exhibition, Society of Petroleum Engineers, Mumbai, India, 2015, p. 8.
[210] D. Wasan, A. Nikolov, K. Kondiparty, The wetting and spreading of nanofluids on solids: role of the structural disjoining pressure, Curr. Opin. Colloid Interface Sci. 16 (2011) 344–349.
[211] T. Phenrat, H.-J. Kim, F. Fagerlund, T. Illangasekare, R.D. Tilton, G.V. Lowry, Particle size distribution, concentration, and magnetic attraction affect transport of polymer-modified Fe0 nanoparticles in sand columns, Environ. Sci. Technol. 43 (2009) 5079–5085.
[212] S.R. Kanel, R.R. Goswami, T.P. Clement, M.O. Barnett, D. Zhao, Two dimensional transport characteristics of surface stabilized zero-valent iron nanoparticles in porous media, Environ. Sci. Technol. 42 (2008) 896–900.
[213] T. Phenrat, N. Saleh, K. Sirk, H.-J. Kim, R.D. Tilton, G.V. Lowry, Stabilization of aqueous nanoscale zerovalent iron dispersions by anionic polyelectrolytes: adsorbed anionic polyelectrolyte layer properties and their effect on aggregation and sedimentation, J. Nanopart. Res. 10 (2008) 795–814.
[214] A. Esfandyari Bayat, R. Junin, A. Samsuri, A. Piroozian, M. Hokmabadi, Impact of metal oxide nanoparticles on enhanced oil recovery from limestone media at several temperatures, Energy Fuels 28 (2014) 6255–6266.
[215] S. Al-Anssari, M. Arif, S. Wang, A. Barifcani, S. Iglauer, Stabilising nanofluids in saline environments, J. Colloid Interface Sci. 508 (2017) 222–229.
[216] E.L. Foster, Z. Xue, C.M. Roach, E.S. Larsen, C.W. Bielawski, K.P. Johnston, Iron oxide nanoparticles grafted with sulfonated and zwitterionic polymers: high stability and low adsorption in extreme aqueous environments, ACS Macro Lett. 3 (2014) 867–871.
[217] M.J. Kadhum, D. Swatske, J. Weston, D.E. Resasco, B. Shiau, J.H. Harwell, Polymer-stabilized multi-walled carbon nanotube dispersions in high-salinity brines, Energy Fuels 31 (2017) 5024–5030.
[218] M. Chorny, I. Fishbein, B.B. Yellen, I.S. Alferiev, M. Bakay, S. Ganta, R. Adamo, M. Amiji, G. Friedman, R.J. Levy, Targeting stents with local delivery of paclitaxel-loaded magnetic nanoparticles using uniform fields, Proc. Natl. Acad. Sci. 107 (2010) 8346–8351.
[219] K.H. Li, B.B. Yellen, Magnetically tunable self-assembly of colloidal rings, Appl. Phys. Lett. 97 (2010) 083105.
[220] K.A. Mirica, S.T. Phillips, C.R. Mace, G.M. Whitesides, Magnetic levitation in the analysis of foods and water, J. Agric. Food. Chem. 58 (2010) 6565–6569.
[221] J. Ge, L. He, J. Goebl, Y. Yin, Assembly of magnetically tunable photonic crystals in nonpolar solvents, J. Am. Chem. Soc. 131 (2009) 3484–3486.
[222] J.S. Andreu, J. Camacho, J. Faraudo, Aggregation of superparamagnetic colloids in magnetic fields: the quest for the equilibrium state, Soft Matter 7 (2011) 2336–2339.
[223] H. Ezzaier, J.A. Marins, C. Claudet, G. Hemery, O. Sandre, P. Kuzhir, Kinetics of aggregation and magnetic separation of multicore iron oxide nanoparticles: effect of the grafted layer thickness, Nanomaterials (Basel, Switzerland) 8 (2018) 623.
[224] G. Verma, P.A. Hassan, Self assembled materials: design strategies and drug delivery perspectives, Phys. Chem. Chem. Phys. 15 (2013) 17016–17028.
[225] H. Chang, T.-T. Tsung, C.-R. Lin, H.-M. Lin, C.-K. Lin, C.-H. Lo, H.-T. Su, A study of magnetic field effect on nanofluid stability of CuO, Key Eng. Mater. 295–296 (2005) 51–56.
[226] M.R. Parker, R.P.A.R. van Kleef, H.W. Myron, P. Wyder, Particle aggregation in colloids in high magnetic fields, J. Magn. Magn. Mater. 27 (1982) 250–256.
[227] K.G. Gareev, I.E. Kononova, V.S. Levitckii, V.A. Moshnikov, S.S. Nalimova, Influence of constant magnetic field on aggregation processes in magnetite colloids, J. Phys. Conf. Ser. 572 (2014) 012027.
[228] M. Wang, L. He, Y. Yin, Magnetic field guided colloidal assembly, Mater. Today 16 (2013) 110–116.
[229] X. Teng, H. Yang, Effects of surfactants and synthetic conditions on the sizes and self-assembly of monodisperse iron oxide nanoparticles, J. Mater. Chem. 14 (2004) 774.
[230] X. Chen, B. Wu, K.W. Jayawardana, N. Hao, S. Jayawaredena, R. Langer, A. Jaklenec, M. Yan, Magnetic multivalent trehalose glycopolymer nanoparticles for the detection of mycobacteria, Adv. Healthcare Mater. 5 (2016).
[231] S. Masur, B. Zingsem, T. Marzi, R. Meckenstock, M. Farle, Characterization of the oleic acid/iron oxide nanoparticle interface by magnetic resonance, J. Magn. Magn. Mater. 415 (2016) 8–12.
[232] L. Li, A. Ruotolo, C.W. Leung, C. Jiang, P. Pong, Characterization and bio-binding ability study on size-controllable highly monodisperse magnetic nanoparticles, Microelectron. Eng. 144 (2015) 61–67.
[233] J. Zhou, Z. Wu, Z. Zhang, W. Liu, Q. Xue, Tribological behavior and lubricating mechanism of Cu nanoparticles in oil, Tribol. Lett. 8 (2000) 213–218.
[234] H. Abdulbari, F. Ling, Drag reduction properties of nanofluids in microchannels, J. Eng. Res. 12 (2015) 60–67.
[235] Y.Y. Wu, M.J. Kao, Using TiO2/DN nanofluid additive for engine lubrication oil, Ind. Lubric. Tribol. 63 (2011) 440–445.
[236] S. Witharana, H. Chen, Y. Ding, Stability of nanofluids in quiescent and shear flow fields, Nanoscale Res. Lett. 6 (2011) 231.
[237] A.R. Pouranfard, D. Mowla, F. Esmaeilzadeh, An experimental study of drag reduction by nanofluids through horizontal pipe turbulent flow of a Newtonian liquid, J. Ind. Eng. Chem. 20 (2014) 633–637.
[238] E.V. Timofeeva, J.L. Routbort, D. Singh, Particle shape effects on thermophysical properties of alumina nanofluids, J. Appl. Phys. 106 (2009) 014304.
[239] B. Kristiawan, S. Kamal, Suhanan, Y. Yanuar, Convective heat transfer of titanium (IV) oxide nanofluids under turbulent flow condition, ARPN J. Eng. Appl. Sci. 10 (2015) 4385–4395.
[240] Z.H. Liu, L. Liao, Forced convective flow and heat transfer characteristics of aqueous drag-reducing fluid with carbon nanotubes added, Int. J. Therm. Sci. 49 (2010) 2331–2338.
[241] A.A. Abdul-Hadi, A.A. Khadom, Studying the effect of some surfactants on drag reduction of crude oil flow, Chinese J. Eng. 2013 (2013) 6.
[242] F.C. Li, Y. Kawaguchi, B. Yu, J.J. Wei, K. Hishida, Experimental study of drag-reduction mechanism for a dilute surfactant solution flow, Int. J. Heat Mass Transf. 51 (2008) 835–843.